

10  
I29A  
489  
cap. 3

UIIU-ENG-81-2002

# ENGINEERING STUDIES

STRUCTURAL RESEARCH SERIES NO. 489



# STOCHASTIC MODELS FOR DEPENDENT LOAD PROCESSES

Metz Reference Room  
Civil Engineering Department  
B106 C.E. Building  
University of Illinois  
Urbana, Illinois 61801

By  
Y. K. WEN  
and  
H. T. PEARCE

A Report to the  
NATIONAL SCIENCE FOUNDATION  
Research Grant CME-79-18053

UNIVERSITY OF ILLINOIS  
at URBANA-CHAMPAIGN  
URBANA, ILLINOIS  
MARCH 1981



STOCHASTIC MODELS FOR DEPENDENT  
LOAD PROCESSES

by

Y. K. Wen

and

H. T. Pearce

A Report to the  
NATIONAL SCIENCE FOUNDATION  
Research Grant CME-79-18053

University of Illinois  
at Urbana-Champaign  
Urbana, Illinois  
March, 1981



<b>REPORT DOCUMENTATION PAGE</b>	1. REPORT NO. UILU-ENG-81-2002	2.	3. Recipient's Accession No.
4. Title and Subtitle Stochastic Models for Dependent Load Processes		5. Report Date March 1981	6.
7. Author(s) Y.K. Wen and H.T. Pearce		8. Performing Organization Rept. No. SRS No. 489	
9. Performing Organization Name and Address Department of Civil Engineering University of Illinois 208 N. Romine Urbana, IL 61801		10. Project/Task/Work Unit No.	11. Contract(C) or Grant(G) No. (C) (G) NSF-CME-79-18053
12. Sponsoring Organization Name and Address National Science Foundation Washington, DC		13. Type of Report & Period Covered	14.
15. Supplementary Notes			
<p>16. Abstract (Limit: 200 words)</p> <p>Stochastic models for dependent loads and load effects are developed. The effects of stochastic dependencies on load combination and structural reliability are investigated in the context of summation of pulse processes in which occurrence time, intensity and duration are allowed to be correlated within each process and between processes. Approximate analytical solutions based on a load coincidence method are obtained and verified by Monte-Carlo simulations. It is found that while within load positive correlations may generally have only moderate effect on the combined load probability, between-load dependencies may be dominant factors and significantly increase the probability of threshold level being exceeded by the combined load.</p>			
<p>17. Document Analysis a. Descriptors Extreme Loads, Natural Hazards, Structural Reliability, Load Combination, Point process, Gauss-Markov sequence, Poisson Delayed process, Bartlett-Lewis process</p> <p>b. Identifiers/Open-Ended Terms</p> <p>c. COSATI Field/Group</p>			
18. Availability Statement Unlimited Distribution	19. Security Class (This Report) Unclassified	21. No. of Pages 78	
	20. Security Class (This Page) Unclassified	22. Price	



## ACKNOWLEDGMENT

This study is supported by the National Science Foundation under grant CME 79-18053. Their support is very much appreciated. Any opinions, findings, and conclusions or recommendations expressed in this report are those of the authors and do not necessarily reflect the views of the National Science Foundation.





## TABLE OF CONTENTS

CHAPTER		Page
I	INTRODUCTION . . . . .	1
	1.1 The Load Model . . . . .	2
	1.2 Method of Load-Coincidence . . . . .	3
II	WITHIN-LOAD DEPENDENCIES . . . . .	6
	2.1 Dependence between Intensity and Duration . . . . .	6
	2.2 Occurrence Dependence (Clustering) . . . . .	8
	2.3 Intensity Dependence . . . . .	15
III	BETWEEN-LOAD DEPENDENCIES . . . . .	21
	3.1 Occurrence Clustering Among Loads . . . . .	21
	3.2 Intensity Dependence Between Loads . . . . .	44
IV	GENERAL CASE . . . . .	50
V	ANALYSIS OF LOAD COINCIDENCE DURATION . . . . .	54
	5.1 Independent Loadings . . . . .	54
	5.2 Dependent Loadings . . . . .	55
VI	SUMMARY AND CONCLUSIONS . . . . .	62
REFERENCES	. . . . .	64
APPENDIX		
A:	Sum of Two Independent Gauss-Markov Processes . . . . .	65
B:	Derivation of Function $h_{12}^{(3)}(t,t')$ . . . . .	67
C:	Integration of Eq. 3.15 . . . . .	69
D:	Monte-Carlo Simulation and Combination of Dependent Pulse Processes . . . . .	70



## LIST OF TABLES

Table		Page
1	Function $f_{T_2-T_1}(\tau)$ . . . . .	25
2	Function $g_2(\mu_{d_1})$ . . . . .	29
3	Comparison of $g_2(\mu_{d_1})$ , $\hat{g}_2(\mu_{d_1})$ with $E[g_2(d_1)]$ . . . . .	30
4	Comparison of $g_{123}$ , $\hat{g}_{123}$ with $E[G_{123}]$ . . . . .	39
5	Coincidence Statistics . . . . .	41
6	Mean Coincidence Duration . . . . .	61



## LIST OF FIGURES

Figure		Page
1	Poisson Renewal Pulse Process . . . . .	4
2	Effect of Load Duration-Intensity Dependence . . . . .	9
3	Bartlett-Lewis Type (Clustered) Pulse Process . . . . .	10
4	Effect of Within-Load Occurrence Clustering . . . . .	14
5	Poisson Renewal Pulse Process with Imbedded Gauss-Markov Intensity . . . . .	16
6	Effect of Within-Load Intensity Dependence . . . . .	20
7	Definition Sketch . . . . .	22
8	Conditional Occurrence Rate (C.O.R.) Function . . . . .	26
9	Two-Time C.O.R. Function $h_{12}^{(3)}(t, t')$ ( $\rho = 2/\text{yr}$ , $a = 10^{-2}\text{yr}$ ) . . . . .	34
10	Coincidence of Three Loads . . . . .	35
11	Probability of Lifetime Combined Maximum ( $P_1 = P_2 = P_3 = 1$ , $\rho_1 = \rho_2 = \rho_3 = 0$ , $\rho = 4$ ) . . . . .	42
12	Probability of Lifetime Combined Maximum ( $P_1 = P_2 = P_3 = 0.5$ , $\rho_1 = \rho_2 = \rho_3 = 2$ , $\rho = 4$ ) . . . . .	43
13	Poisson Renewal Pulse Processes with Correlated Intensities . . . . .	45
14	Effect of Between-Load Intensity Dependence . . . . .	49
15	Within- and Between-Load Occurrence Clustering . . . . .	51
16	Effect of Load Correlation in both Intensity and Occurrences . . . . .	53
17	Coincidence Duration for Independent Pulse Processes . . . . .	56
18	Condition that Process $S_1(t)$ and $S_2(t)$ are "on" at $t = t_0$ . . . . .	58
19	Comparison of Correlation Coefficient Functions . . . . .	66



## I. INTRODUCTION

Recently, largely due to stringent safety requirements for important structures in extreme environments such as nuclear power plants and offshore platforms, there has been a fast growing interest in the risk analysis of low-probability and large-consequence events such as combination of a number of unfavorable loading conditions producing catastrophic consequences. Significant progress has been made in the last few years in the modeling and combination of stochastic loadings that the research findings are beginning to be used in the formulation of design requirements in building codes. However, so far, efforts have been concentrating on the combination of independent loadings i.e. the time of load occurrence, intensity and duration given load occurrence are assumed to be statistically independent of one another in each occurrence, from occurrence to occurrence and from loading to loading in each loading. In reality, these variables may be correlated. For example, a single severe storm may produce extreme wind, wave, snow, surge and temperature loads, earthquakes may cause direct dynamic force, indirect fire load and in a nuclear structure, loss-of-coolant accident (LOCA) loadings because of pipe break, etc. What would be the effect of such dependencies on the probability of combined load and lifetime reliability estimate of structures?

The purpose of this study is to develop stochastic models for correlated load processes and examine the effects of load dependencies on the probability of combined load and reliability of structures under such loadings.

Based on a pulse load model, the occurrence (time) dependencies are introduced using multi-variate Poisson delayed point process and point process of the Bartlett-Lewis type; the intensity dependencies are introduced using an imbedded Gauss-Markov sequence and "conditional" correlation function matrix;

and the duration-intensity dependencies are introduced using multi-variate distribution. The load coincidence method previously proposed (11,12,13) for independent loading is generalized for the combination analysis of dependent loads. Approximate analytical results are obtained in simple, closed form. The accuracies of the analytical solutions are verified by extensive Monte-Carlo simulations. (Details of simulation given in Appendix D).

### 1.1 The Load Model

Because of the randomness in their occurrence time, intensity and duration, time varying loadings need to be modeled as random processes. If the loading fluctuation over the structure's lifetime can be modeled as stationary Gaussian processes, the dependences between load can be properly accounted for by the cross-correlation functions and linear combination of the loadings can be handled without difficulty. One can take advantage of the fact that the combined process is again Gaussian and for which many useful results such as upcrossing rate and first-passage probability have been obtained and can be directly used in the evaluation of probability of combined load and structural reliability. Unfortunately, for many loadings, (such as those caused by storms and earthquakes), this is not the case because of their transient and intermittent nature.

A simple and flexible model for the macro-time fluctuation of loadings is the pulse process in which the occurrence time is modeled by a point process, and the duration and intensity given occurrence by random variables. For example, the Poisson renewal pulse process is widely used for transient loads characterized by a mean occurrence rate  $\lambda$ , a mean load duration  $\mu_d$ , a specified pulse shape (rectangular, triangular, etc.) and a random intensity (7,11,12). In most previous studies load parameter independences have been assumed; herein, such restriction is relaxed (i.e. the duration may be dependent



on the intensity, the occurrence may not be a simple Poisson process, etc.). Such models, although being rather crude and idealized, do capture the essential macro-scale properties of time-varying loads and allow tractable analytical solutions, therefore insights to be gained into this complex problem.

Sample functions of rectangular pulse load processes are shown in Fig. 1. For a Poisson renewal pulse process, the load changes occur according to a Poisson process with a mean rate of  $1/\mu_d$ . Given the change there is a probability of  $\lambda\mu_d$  that the load has a non-zero intensity. Therefore, the non-zero part of the process has an arrival rate of  $\lambda$  and durations governed by an exponential distribution with a mean value of  $\mu_d$ . In other words, at a given arbitrary instant of time the load intensity density function has a discrete mass of  $(1-\lambda\mu_d)$  at zero, indicating the fraction of the time the load is "off." When  $\lambda\mu_d=1$ , the load is always "on" (Fig. 1b), i.e. a Poisson square wave; when  $\lambda\mu_d<1$ , the load may be "off" from time to time (Fig. 1a). Most transient loads have a  $\lambda\mu_d < 0.015$  (9). More details are available in Larrabee (7).

## 1.2 Method of Load-Coincidence

The general problem of lifetime reliability of structure under multiple time-varying loadings is extremely complex. A rigorous formulation requires a first-excursion time probability analysis of a vector process (loadings) out of a general nonlinear safe domain (limit state). An approximate solution can be obtained based on the consideration that survival of the structure (limit state not being reached in the structure's lifetime) requires survival under individual loadings as well as coincidence of two or more loadings. Therefore, for independent loadings modeled as Poisson pulse processes the structural reliability is (11,12,13)

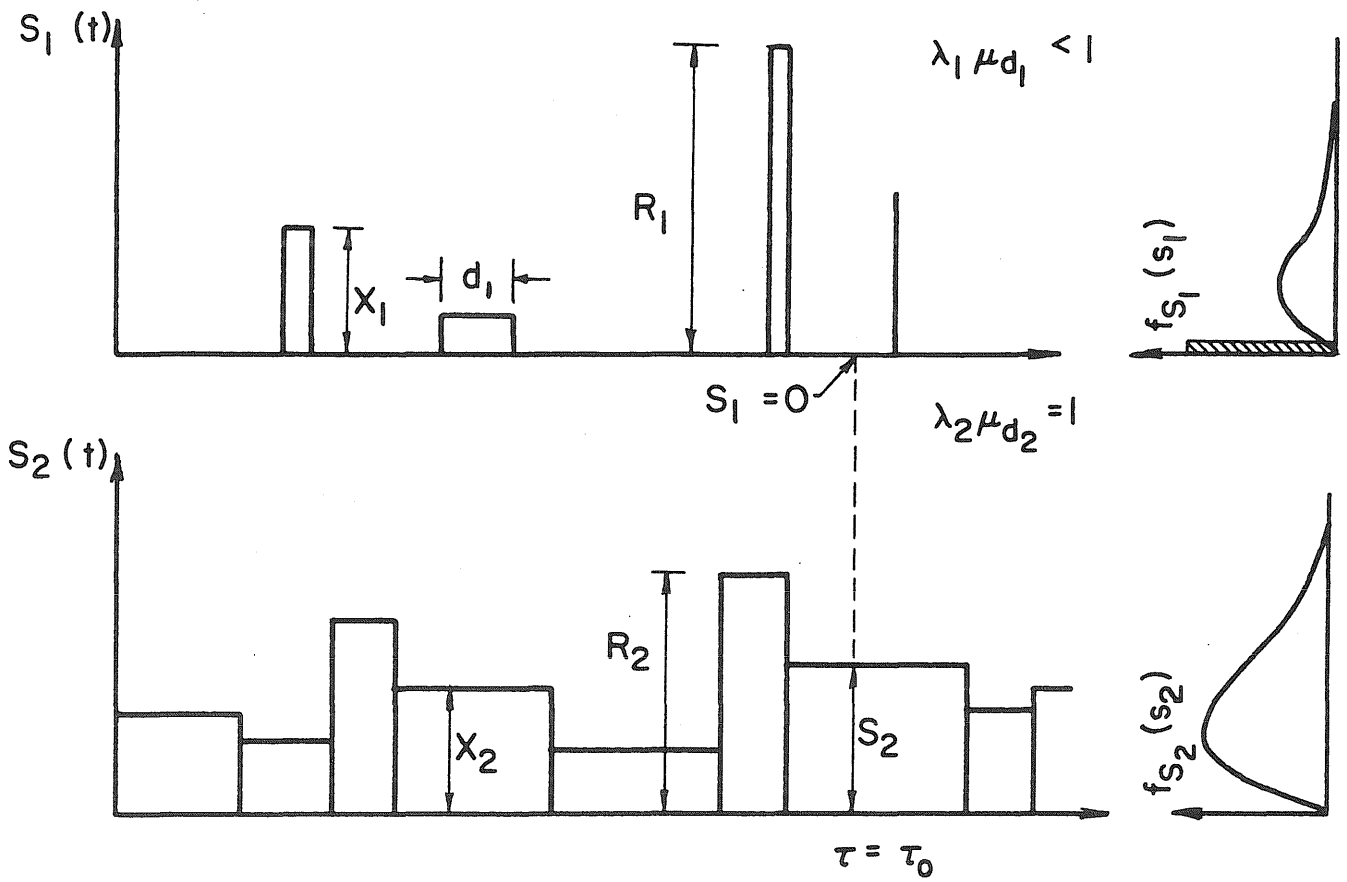


Fig. 1 Poisson Renewal Pulse Process

$$1 - P_f \approx \exp[-\sum_{i=1}^N \lambda_i P_i^m t - \sum_{i \neq j}^N \sum^N \lambda_{ij} P_{ij}^m t - \sum_{i \neq j \neq k}^N \sum^N \sum^N \lambda_{ijk} P_{ijk}^m t + \dots] \quad (1.1)$$

in which

$\lambda_i \approx \lambda_i$ ,  $\lambda_{ij} \approx \lambda_i \lambda_j (\mu_{d_i} + \mu_{d_j})$ ,  $\lambda_{ijk} \approx \lambda_i \lambda_j \lambda_k (\mu_{d_i} \mu_{d_j} + \mu_{d_j} \mu_{d_k} + \mu_{d_i} \mu_{d_k})$  are the mean rate of occurrence of load  $S_i(t)$  only, coincidence of load  $S_i(t)$  and  $S_j(t)$  only and coincidence of  $S_i(t)$ ,  $S_j(t)$ , and  $S_k(t)$  only, etc.  $P_i^m$ ,  $P_{ij}^m$  and  $P_{ijk}^m$  are the conditional probability of failure (mth limit state being reached) given the occurrence and coincidence of loads, respectively. The above formulation is generally conservative, applicable to linear, nonlinear, static and dynamic systems and its accuracy has been verified by extensive Monte-Carlo simulations. Details are available in Refs. 11, 12, and 13. In the following, the method is extended to the combination of dependent loadings.

Other methods, such as those based on an upcrossing rate analysis have been developed for linear combination of independent load processes (7,8), however, extension of these methods to dependent loadings appears to be difficult.

For simplicity, only the linear combination (summation) of rectangular pulse processes is considered. The limit state is a given threshold level  $r$  being exceeded. Therefore, Eq.1.1 gives the probability that such level is not exceeded in  $(0,t)$   $P_i^m$ ,  $P_{ij}^m$ , and  $P_{ijk}^m$  reduce to  $G_i^*(r)$ ,  $G_{ij}^*(r)$ , and  $G_{ijk}^*(r)$ , the conditional probabilities of  $r$  being exceeded given the occurrence and coincidence of loads, respectively. To isolate the effect of each dependence, when the dependence involving certain load parameters is considered other parameters are assumed to be statistically independent. The dependencies are categorized into those which are primarily within-load or between-load.

## II. WITHIN-LOAD DEPENDENCES

Loads under combination are assumed to be statistically independent of one another, however, occurrence, intensity and duration within each load may be correlated.

### 2.1 Dependence between Intensity and Duration

For example, storms with longer duration usually have higher intensity, therefore, these two parameters may be correlated within each load. The occurrence times are assumed to be statistically independent, i.e. they can be modeled by Poisson processes. The contribution to the lifetime combined maximum from individual load will not be affected by this dependence since it does not involve duration i.e. the single summation terms in Eq. (1.1) remains the same. However, the coincidence term would be affected since the condition of coincidence implies higher chance of longer duration, hence, higher intensities and probability of threshold being exceeded. The coincidence term for the combination of two loads is derived as follows.

Let  $R$  be the combined load,  $X_i$  be the intensity given the occurrence of load  $S_i(t)$ . The probability that two loads coincide and  $R$  exceeds a given threshold level  $r$  in a given time interval  $(t, t+\Delta t)$  is

$$P = P(R > r | E_1) P(E_1) + P(R > r | E_2) P(E_2) \quad (2.1)$$

in which  $E_1$  = that  $S_1(t)$  and  $S_2(t)$  coincide and  $S_1(t)$  is "on" first

$E_2$  = that  $S_1(t)$  and  $S_2(t)$  coincide and  $S_2(t)$  is "on" first

and

$$P(E_1) \approx \lambda_1 \Delta t \lambda_2 \mu_{d_1} \quad (2.2)$$

$$P(E_2) \approx \lambda_2 \Delta t \lambda_1 \mu_{d_2}$$

The above is true since the load occurrences are modeled by independent Poisson processes.

$$P(R > r | E_1) = \int P(X_1 + X_2 > r | \hat{D}_1 = d_1) f_{\hat{D}}(d_1) d d_1 \quad (2.3)$$

in which  $\hat{D}_1$  = duration of  $S_1(t)$  given  $E_1$ .

$$f_{\hat{D}}(d_1) = \frac{d_1 f_{D_1}(d_1)}{\mu_{d_1}} \quad (2.4)$$

where  $D_1$  = duration of  $S_1(t)$ , an exponential variate with a mean  $= \mu_{d_1}$ .

Intuitively, given the event  $E_1$  (that is, the duration of  $S_1(t)$  covers the occurrence time of  $S_2(t)$ ), the duration  $D_1$  would be more likely to be longer, the well-known waiting time paradox (4). The relation given by Eq. 2.4 can be found in Ref. 3. Therefore,

$$\begin{aligned} P(R > r | E_1) &= 1 - \int_0^{\infty} \left[ \int_0^r F_{X_2}(r-x_1) f_{X_1|d_1}(x_1) dx_1 \right] \frac{d_1 f_{D_1}(d_1)}{\mu_{d_1}} d d_1 \\ &= 1 - \int_0^{\infty} \int_0^r \frac{d_1}{\mu_{d_1}} F_{X_2}(r-x_1) f_{X_1, D_1}(x_1, d_1) dx_1, dd_1 \end{aligned} \quad (2.5)$$

in which  $f_{X_1, D_1}$  = joint density function of  $X_1$  and  $D_1$ . Similarly,

$P(R > r | E_2)$  can be obtained. The mean rate of threshold level  $r$  being exceeded due to the coincidence is therefore,

$$\begin{aligned} P/\Delta t &= \lambda_1 \lambda_2 \mu_{d_1} \left[ 1 - \int_0^{\infty} \int_0^r \frac{d_1}{\mu_{d_1}} F_{X_2}(r-x_1) f_{X_1, D_1}(x_1, d_1) dx_1, dd_1 \right] + \\ &\quad \lambda_1 \lambda_2 \mu_{d_2} \left[ 1 - \int_0^{\infty} \int_0^r \frac{d_2}{\mu_{d_2}} F_{X_1}(r-x_2) f_{X_2, D_2}(x_2, d_2) dx_2, dd_2 \right] \end{aligned} \quad (2.6)$$

Note that when the duration and intensity are independent the above coincidence term reduces to

$$\lambda_1 \lambda_2 (\mu_{d_1} + \mu_{d_2}) [1 - F_{X_{12}}(r)] \quad (2.7)$$

in which  $X_{12} = X_1 + X_2$ . Eq. 2.7 agrees with the coincidence term in Eq. 1.1.

If  $X_i$  and  $D_i$  are jointly normal, the double integration in Eq. 2.6 can be reduced to

$$\int_0^{\infty} F_{X_j}(r-x_i) f_{X_i}(x_i) \left[ 1 + \rho_i \frac{\sigma_{d_i}}{\sigma_{X_i}} \left( \frac{x_i}{\mu_{d_i}} - \frac{\mu_{X_i}}{\mu_{d_i}} \right) \right] dx_i \quad (2.8)$$

in which  $\mu_{X_i} = E[X_i]$ ,  $\sigma_{X_i}$  = standard deviation of  $X_i$  and  $\sigma_{d_i}$  = standard deviation of  $D_i$ .  $\rho_i$  = correlation coefficient between  $X_i$  and  $D_i$ . Eq. 2.8 can be used as an approximation when  $X_i$  and  $D_i$  are not jointly Gaussian.

To see the effect of the dependence, the ratio of Eq. 2.6 to the coincidence term for independent  $X_i$  and  $D_i$  are plotted for  $\rho = 0.5$  and  $1.0$  in Fig. 2 for  $X_i$  and  $D_i$  jointly normal and jointly gamma.  $\mu_{X_i} = \mu_{d_i} = 1.0$ ,  $\sigma_{X_i} = \sigma_{d_i} = 0.3$ . It is seen that the ratio increases with the threshold level, reaching a factor about 2 for very high level. This corresponds approximately to the error factor that the risk would be underestimated since at such levels, the coincidence term dominates the distribution. Note that in this case the difference in threshold levels for a fixed risk of being exceeded would be small. Similar results based on a point crossing rate method have been found in Ref. 7.

## 2.2 Occurrence Dependence (Clustering)

A common phenomenon of occurrence dependence is clustering; examples are main and after shocks of earthquake, a large number of tornadoes spawned by a single storm, etc. Such dependence is modeled by a point process of the Bartless-Lewis (1) type shown in Fig. 3. The load occurs in clusters which are modeled as a Poisson renewal process with a mean rate of occurrence  $\lambda_{c_i}$  and a mean cluster length (duration)  $\mu_{c_i}$ . Within each cluster, the loading is a Poisson renewal pulse process with a mean duration  $\mu_{d_i}$  and

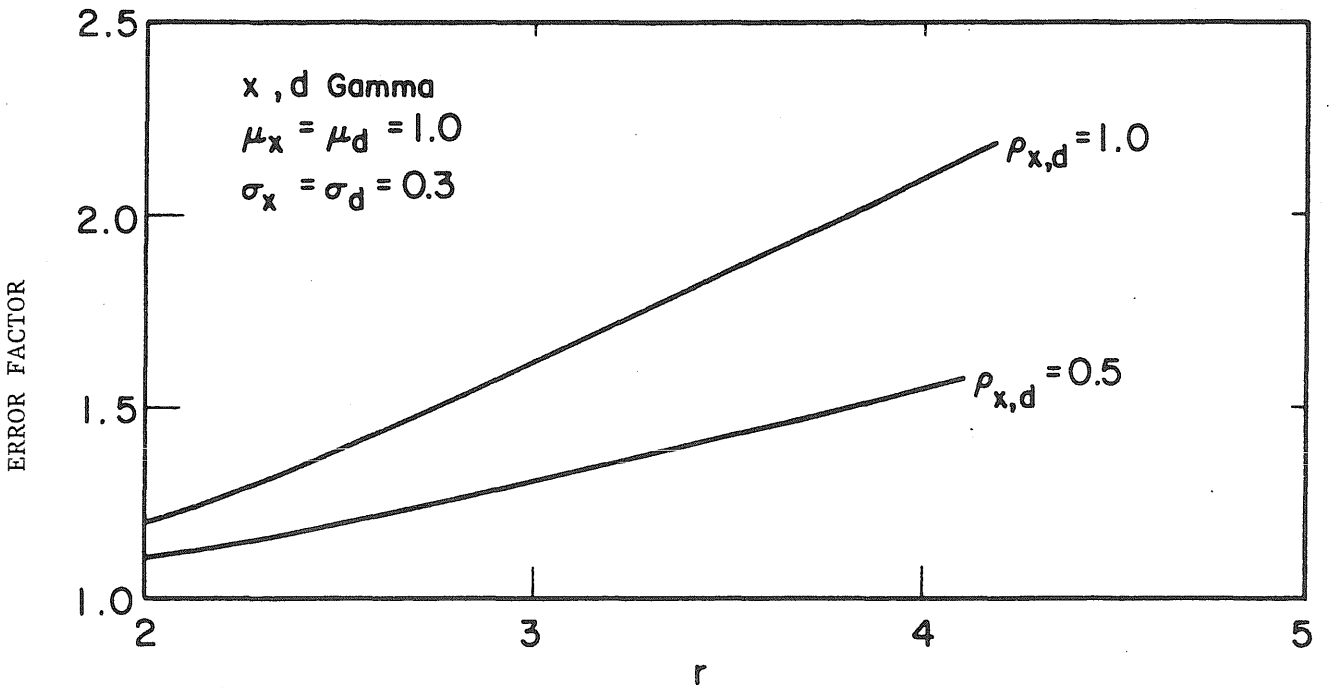
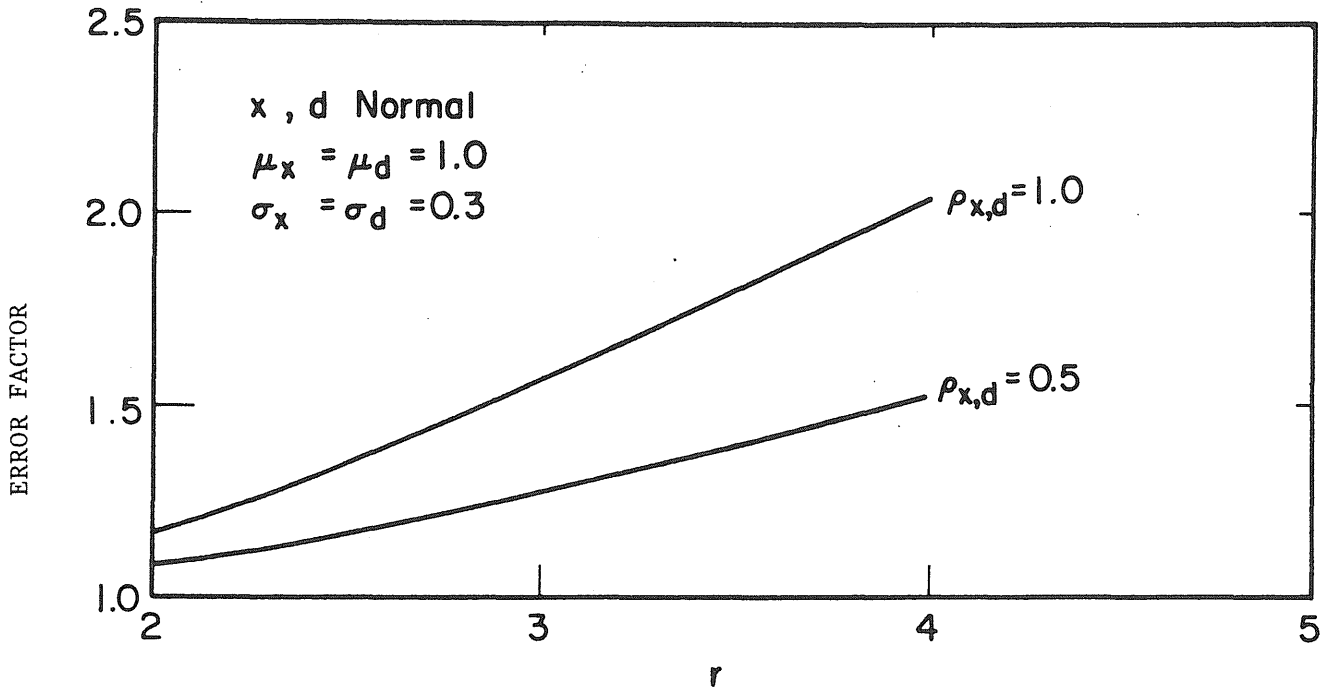
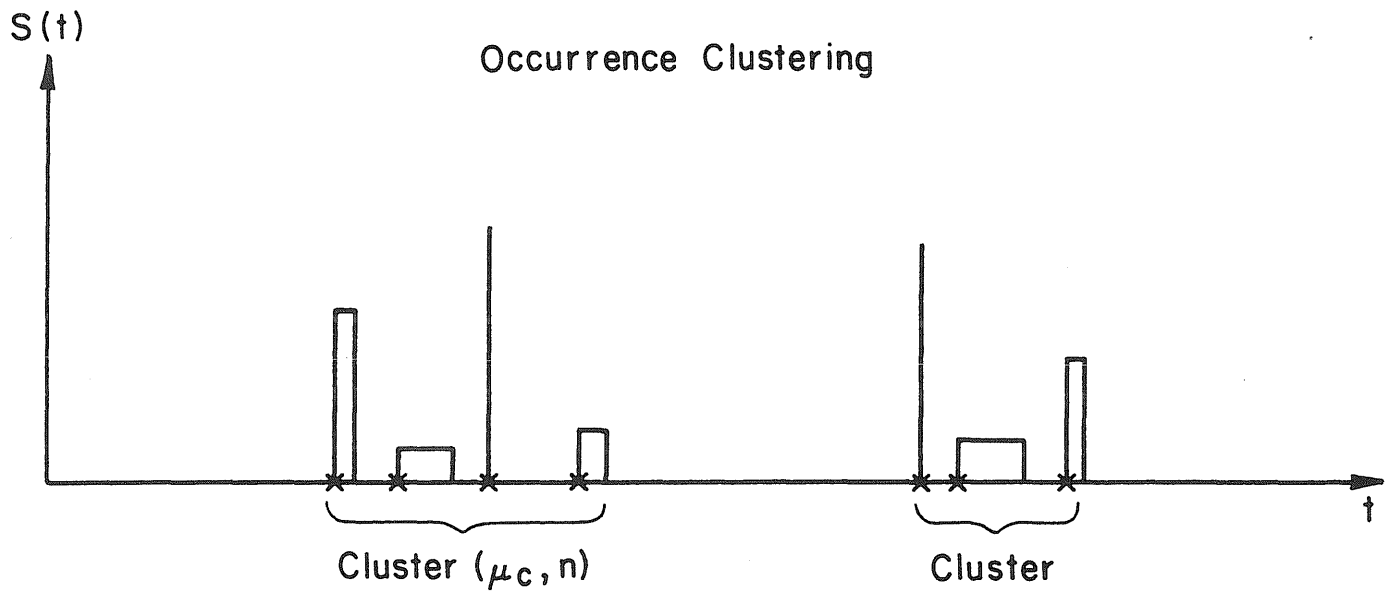


Fig. 2 Effect of Load Duration-Intensity Dependence



\* = Bartlett-Lewis Cluster Process

$\mu_c$  = Mean Cluster Duration

$n$  = Mean No. of Occurrences/Cluster

Fig. 3 Bartlett-Lewis Type (Clustered)  
Pulse Process



an occurrence rate  $n_i/\mu_{c_i}$  in which  $n_i$  = the mean number of occurrence per cluster. The occurrence rate of loading over the lifetime is therefore  $\lambda_i = \lambda_{c_i} n_i$ . Duration and intensity are assumed to be independent of each other and also independent of the occurrence time.

Because of the clustering, the counting of the load occurrences in the lifetime of the structure is no longer governed by a Poisson distribution, i.e. it follows approximately a negative binomial distribution. As a result, Eq. 1.1 will be modified. Let  $R_i$  be the lifetime maximum value of  $S_i(t)$ , the probability distribution of  $R_i$  can be derived as follows. Consider load  $S_i(t)$ .

$$P(R_1 \leq r) = \sum_{k=0}^{\infty} P(R \leq r) | N_c = k) P(N_c = k) \quad (2.9)$$

in which  $N_c$  = number of clusters. Since within each cluster, the load is still a Poisson renewal process, given  $N_c=k$  and the total duration of the "on" time of the clusters, to

$$P(R_1 \leq r) | N_c=k, t_0) = e^{-n_1/\mu_{c_1} [1-F_{X_1}(r)] t_0} \quad (2.10)$$

in which  $t_0 = t_1+t_2+\dots+t_k$ ,  $t_i$ =the duration of the  $i$ th cluster.

$(t_1, t_2, \dots, t_k)$  is a subset of  $(t_1', t_2', \dots, t_n')$   $n \geq k$  uniformly distributed for  $\sum_{i=1}^n t_i' \leq T$  and zero otherwise. As an approximation, if the condition  $N_c=k$  is disregarded,  $t_i$  are independently exponential distribution and  $t_0$  is a gamma variate with a density function

$$f_{T_0}(t_0) = \frac{1}{\mu_{c_1}} \frac{\left(\frac{t_0}{\mu_{c_1}}\right)^{k-1}}{(k-1)!} e^{-t_0/\mu_{c_1}} \quad (2.11)$$

therefore

$$P(R_1 \leq r | N_c=k) \approx \int_0^{\infty} P(R \leq r | N_c=k, t_0) f_{T_0}(t_0) dt_0$$

$$= \left[ \frac{1}{n_1 [1 - F_{X_1}(r)] + 1} \right]^k \quad (2.12)$$

Substituting Eq. 2.12 into Eq. 2.9 one obtains

$$\begin{aligned} P(R_1 \leq r) &\approx \sum_{k=0}^{\infty} \left\{ \frac{1}{n_1 [1 - F_{X_1}(r)] + 1} \right\}^k \frac{(\lambda_{c_1} t)^k}{k!} e^{-\lambda_{c_1} T} \\ &= \exp\left\{-\lambda_{c_1} T \left[ \frac{n_1 F_{X_1}^*(r)}{n_1 F_{X_1}^*(r) + 1} \right]\right\} \end{aligned} \quad (2.13)$$

in which  $F_{X_1}^*(r) = 1 - F_{X_1}(r)$ . Similarly, probability distribution of the lifetime maximum of  $S_2(t)$ ,  $R_2$ , can be obtained.

Since the clusters are modeled as Poisson renewal processes, the coincidence of clusters is also Poissonian with a mean rate of (11)

$$\lambda_{12}^c \approx \lambda_{c_1} \lambda_{c_2} (\mu_{c_1} + \mu_{c_2}) \quad (2.14)$$

Within each overlap of clusters, the load coincidence is again a Poisson process with a mean rate of

$$\lambda_{12} \approx \frac{n_1 n_2}{\mu_{c_1} \mu_{c_2}} (\mu_{d_1} + \mu_{d_2}) \quad (2.15)$$

Let  $R_{12}$  be the lifetime maximum of the coincidence part of the combined process

$$P(R_{12} \leq r) = \sum_{k=0}^{\infty} P(R_{12} < r | N_{cc} = k) P(N_{cc} = k) \quad (2.16)$$

in which  $N_{cc}$  = number of cluster coincidences. With the total duration of cluster overlaps approximated by a gamma variate one obtains, similar to Eq. 2.12,

$$P(R_{12} \leq r | N_{cc} = k) \approx \left[ \frac{1}{\lambda_{12} \mu_{c_{12}} [1 - F_{X_{12}}(r)] + 1} \right]^k \quad (2.17)$$

in which  $X_{12} = X_1 + X_2$ , the combined intensity given the load coincidence.

Therefore,

$$P(R_{12} \leq r) \approx \exp\{-\lambda_{12}^c t \left[ \frac{\lambda_{12} \mu_{c12} F_{X_{12}}^*(r)}{\lambda_{12} \mu_{c12} F_{X_{12}}(r) + 1} \right]\} \quad (2.18)$$

Let  $R_m$  = the lifetime combined maximum

$$\begin{aligned} P(R_m \leq r) &= P(R_1 \leq r \cap R_2 \leq r \cap R_{12} \leq r) \\ &\approx P(R_1 \leq r) P(R_2 \leq r) P(R_{12} \leq r) \end{aligned} \quad (2.19)$$

$R_1$  is independent of  $R_2$ ; however,  $R_{12}$  strictly speaking, is positively correlated to  $R_1$  and  $R_2$ , therefore, the above approximation is on the conservative side. Substituting Eqs. 2.13 and 2.18 into 2.19, one obtains

$$\begin{aligned} F_{R_m}(r, T) &\approx \exp\{-\lambda_1 T F_{X_1}^*(r) \left[ \frac{1}{n_1 F_{X_1}^*(r) + 1} \right] - \lambda_2 T F_{X_2}^*(r) \left[ \frac{1}{n_2 F_{X_2}^*(r) + 1} \right] \\ &\quad - \lambda_{12} T F_{X_{12}}^*(r) \left[ \frac{1}{n_1 n_2 \left( \frac{\mu_{d1} + \mu_{d2}}{\mu_{c1} + \mu_{c2}} \right) F_{X_{12}}^*(r) + 1} \right]\} \end{aligned} \quad (2.20)$$

in which  $\lambda_{12} \approx \lambda_1 \lambda_2 (\mu_{d1} + \mu_{d2})$ . Comparison with the independent loading case shows that the effect of the clustering is accounted for by the terms in the square bracket which is important when  $n_i$  is large and the threshold level  $r$  is low. In Fig. 4,  $F_{R_m}$  for the clustered and unclustered cases are compared. The loading parameters are  $\lambda_1 = \lambda_2 = \lambda = 6/\text{year}$ .  $\mu_{c1} = \mu_{c2} = 0.01 \text{ yr}$  ( $\approx 3 \text{ days}$ ),  $\mu_{d1} = \mu_{d2} = 0.001 \text{ yr}$  ( $\approx 8 \text{ hrs}$ ).  $X_1$  and  $X_2$  are normal with  $\mu_{X_1} = \mu_{X_2} = 1.0$  and  $\sigma_{X_1} = \sigma_{X_2} = 0.3$ . The rest are indicated in the figure. Monte-Carlo simulation results are also shown; they agree very well with the analytical solutions. It is seen that as threshold level increases, the effect of clustering on the distribution function diminishes. This is what one would expect since crossings tend to be sparse and independent at high

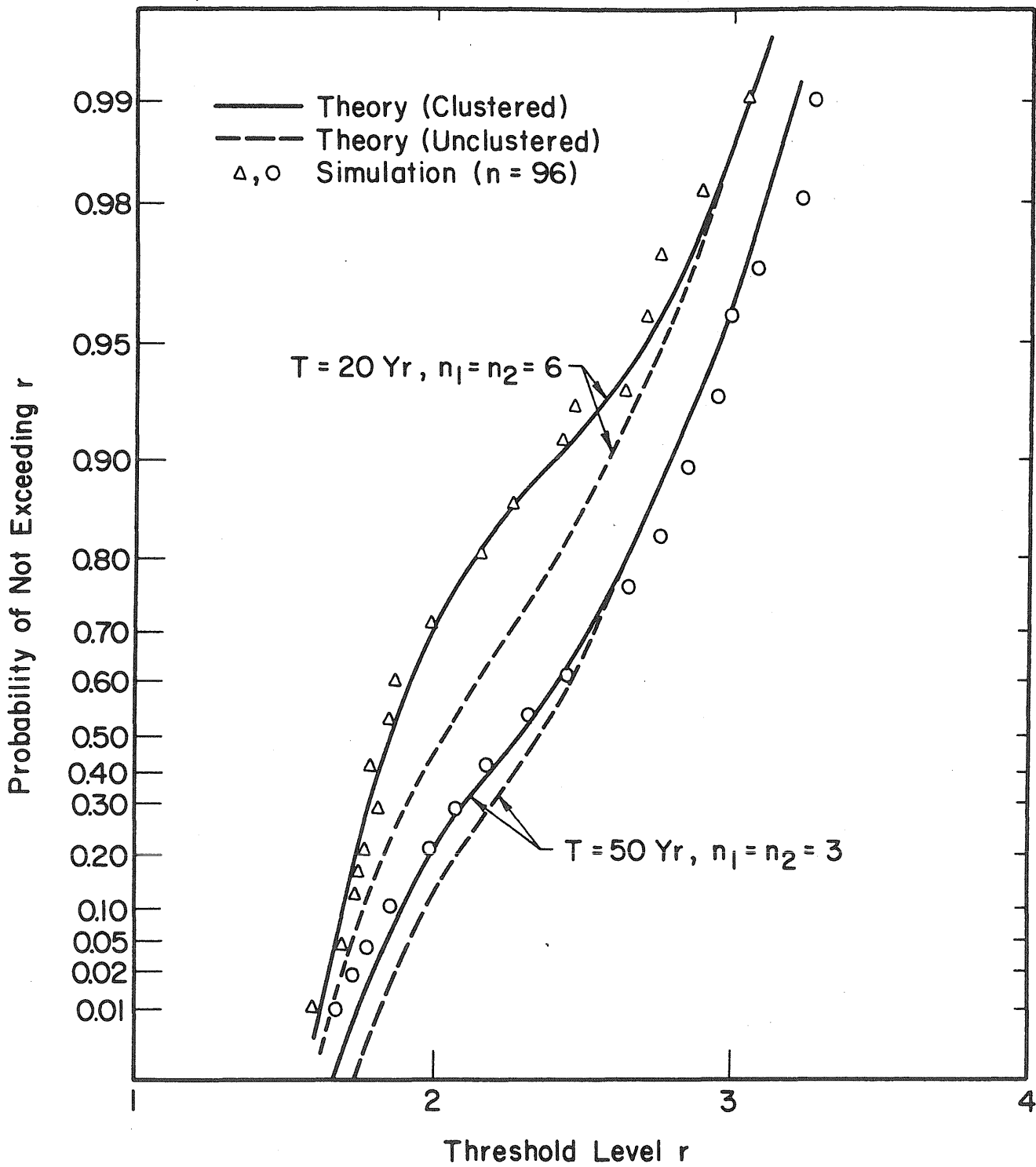


Fig. 4 Effect of Within-Load Occurrence Clustering

threshold levels even for clustered load process. The overall effect of clustering can be described as only moderate and give lower lifetime combined maximum compared with the independent loadings case.

### 2.3 Intensity Dependence

The Gauss-Markov sequence is a simple and flexible model to include dependence, for example such model has been used in a study of effect of intensity correlation on structural safety (5). In this study, this is done by imbedding such a sequence in a Poisson renewal pulse process (see Fig. 5). In other words, the intensities given occurrence are related by

$$X_{k+1} = \rho X_k + \sqrt{1-\rho^2} Z_k \quad (2.21)$$

in which  $X_i$  = intensity at  $i$ th occurrence.  $Z_k$  = independent normal variate with  $\mu_Z = \sqrt{(1-\rho)/(1+\rho)} \mu_X$ , and  $\sigma_Z = \sigma_X$ . The intensity correlation is

$$\rho_{X_j, X_k} = \rho^{|j-k|} \quad (2.22)$$

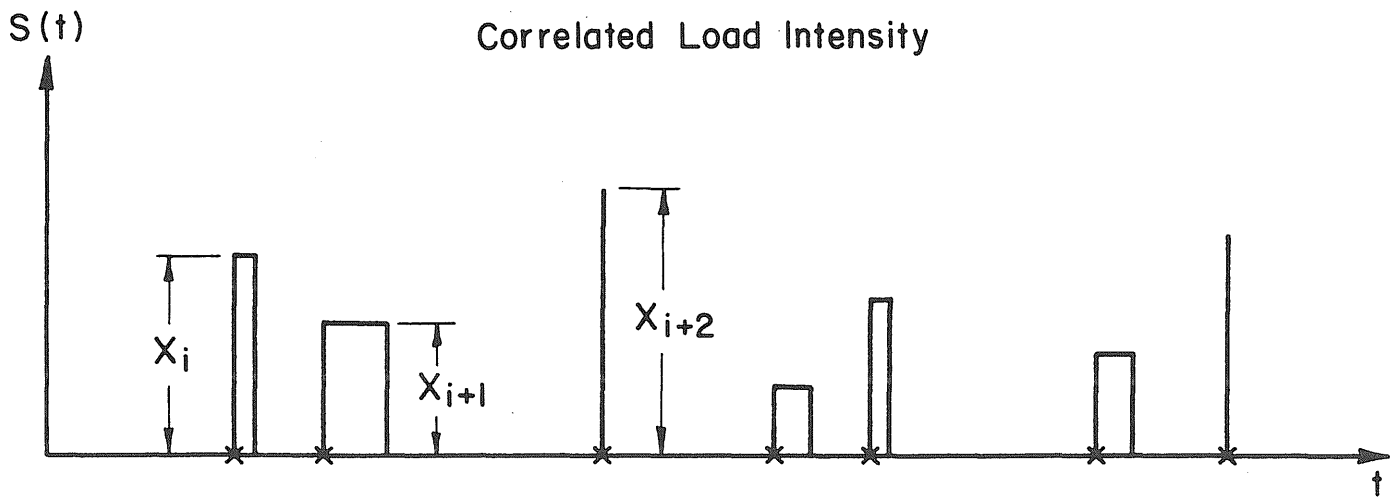
in which  $\rho_{X_j, X_k}$  is the correlation coefficient between the intensities at the  $j$ th and  $k$ th occurrence.

Following the notations used in Section 2.2

$$P(R_1 \leq r) = \sum_{k=0}^{\infty} P(R_1 \leq r | N_1=k) P(N_1=k) \quad (2.23)$$

in which  $N_1$  = number of occurrences.

$$\begin{aligned} P(R_1 \leq r | N_1=k) &= P[X_1^{(1)} \leq r \cap X_2^{(1)} \leq r \dots X_k^{(1)} \leq r] \\ &= P[X_k^{(1)} \leq r | X_{k-1}^{(1)} \leq r] P[X_{k-1}^{(1)} \leq r | X_{k-2}^{(1)} \leq r] \dots \\ &\quad \dots P[X_1^{(1)} \leq r] \end{aligned}$$



$X_{i-1}, X_i, X_{i+1}, \dots =$  Gauss-Markov Sequence  
 x = Poisson Process

Fig. 5 Poisson Renewal Pulse Process with Imbedded Gauss-Markov Intensity

$$= \begin{cases} [H_1(r, \rho_1)]^{k-1} P(X_1^{(1)} \leq r) & \text{for } k \geq 1 \\ 1 & \text{for } k=0 \end{cases} \quad (2.24)$$

in which  $H_1(r, \rho_1)$  = conditional probability that the intensity  $X_i^{(1)} \leq r$  given the intensity at the previous occurrence  $X_{i-1}^{(1)} \leq r$ .

The above is true because of the Markov property of the sequence  $X_i^{(1)}$ .

Substituting Eq. 2.24 into Eq. 2.23 one obtains,

$$P(R_1 \leq r) = \frac{F_{X_1^{(1)}}(r)}{H_1(r, \rho_1)} \{ e^{-\lambda_1 T H_1^*(r, \rho_1)} - e^{-\lambda_1 T} \} + e^{-\lambda_1 T} \quad (2.25)$$

in which  $H_1^* = 1 - H_1$ .

The function  $H_1(r, \rho_1)$  is given by

$$\begin{aligned} H_1(r, \rho_1) &= P(X_i^{(1)} \leq r | X_{i-1}^{(1)} \leq r) \\ &= \int_0^r \frac{P(X_i^{(1)} \leq r | X_{i-1}^{(1)} = s)}{P(X_{i-1}^{(1)} \leq r)} f_{X_{i-1}^{(1)}}(s) ds \end{aligned} \quad (2.26)$$

in which  $P(X_i^{(1)} \leq r | X_{i-1}^{(1)} = s)$

$$\begin{aligned} &= P(\rho_1 s + \sqrt{1-\rho_1^2} Z_{i-1} \leq r) \\ &= F_Z \left[ \frac{1}{\sqrt{1-\rho_1^2}} (r - \rho_1 s) \right] \end{aligned}$$

Therefore,

$$H_1(r, \rho_1) = \frac{\int_0^r F_Z \left[ \frac{1}{\sqrt{1-\rho_1^2}} (r - \rho_1 s) \right] f_{X_1^{(1)}}(s) ds}{F_{X_1^{(1)}}(r)} \quad (2.27)$$

Consider now the lifetime maximum due to the load coincidence. The coincidence part has intensity variation which is the sum of parts of two independent Markov sequences. It can be shown that the sum of two stationary Gauss-Markov

sequences is again Markovian when the one-step correlation coefficients are equal; otherwise, the sum sequence is strictly no longer Markovian, however, with a correlation structure very close to that in a Markov sequence (Appendix A). Therefore, the coincidence intensity sequence can be treated approximately as being Markovian.

Let  $Y_p = X_i^{(1)} + X_j^{(2)}$ ,  $Y_{p+1} = X_{i+k}^{(1)} + X_{j+l}^{(2)}$ , etc. be the intensity sequence. It can be easily shown that

$$\rho_{p,p+1} = (\rho_1^k \sigma_{X^{(1)}}^2 + \rho_2^l \sigma_{X^{(2)}}^2) / (\sigma_{X^{(1)}}^2 + \sigma_{X^{(2)}}^2) \quad (2.28)$$

Therefore, the correlation coefficient between two adjacent intensities in the sum sequence is no longer constant. As an approximation, an equivalent constant value for the one-step correlation coefficient is used.

$$\rho_{12} \approx \frac{\rho_1^{\lambda_1/\lambda_{12}} \sigma_{X^{(1)}}^2 + \rho_2^{\lambda_2/\lambda_{12}} \sigma_{X^{(2)}}^2}{\sigma_{X^{(1)}}^2 + \sigma_{X^{(2)}}^2} \quad (2.29)$$

in which  $\lambda_1/\lambda_{12} = \lambda_1/[\lambda_1\lambda_2(\mu_{d_1} + \mu_{d_2})]$ , the mean number of load occurrences in  $S_1(t)$  between two adjacent coincidences.  $\lambda_2/\lambda_{12}$  is similarly defined. Following a procedure similar to that which lead to Eq. 2.25, one obtains the distribution function for  $R_{12}$  as

$$P(R_{12} \leq r) \approx \frac{F_{X_{12}}(r)}{H_{12}(r, \rho_{12})} \{ e^{-\lambda_{12} T H_{12}^*(r, \rho_{12})} - e^{-\lambda_{12} T} \} + e^{-\lambda_{12} T} \quad (2.30)$$

in which

$$H_{12}(r, \rho_{12}) = \frac{\int_0^r F_{Z_{12}} \left[ \frac{1}{\sqrt{1-\rho_{12}^2}} (r-\rho_{12}s) \right] f_{X_{12}}(s) ds}{F_{X_{12}}(r)} \quad (2.31)$$

with  $X_{12} = X^{(1)} + X^{(2)}$ , the combined intensity,  $Z_{12}$  = normal variate with  $\mu_Z = \sqrt{(1-\rho_{12}^2)/(1+\rho_{12}^2)} \mu_{X_{12}}$  and  $\sigma_{Z_{12}} = \sigma_{X_{12}}$ .



The overall lifetime combined maximum therefore has the following approximate distribution:

$$F_{R_m}(r, T) \approx P(R_1 \leq r) P(R_2 \leq r) P(R_{12} \leq r) \quad (2.32)$$

Terms  $e^{-\lambda_1 T}$ ,  $e^{-\lambda_2 T}$  and  $e^{-\lambda_{12} T}$  are usually small and can be neglected. If  $\rho_1$ ,  $\rho_2$  and  $\rho_{12} \Rightarrow 0$ , the dependencies disappear; Eq. 2.32 reduces to Eq. 1.1. If  $\rho_1$ ,  $\rho_2$  and  $\rho_{12} \Rightarrow 1$ ; Eq. 2.32 reduces to

$$F_{R_m}(r, T) \approx \{F_{X(1)}(r) [1 - e^{-\lambda_1 T}] + e^{-\lambda_1 T}\} \{F_{X(2)}(r) [1 - e^{-\lambda_2 T}] + e^{-\lambda_2 T}\} \\ \{F_{X_{12}}(r) [1 - e^{-\lambda_{12} T}] + e^{-\lambda_{12} T}\} \quad (2.33)$$

which can be also obtained from the fact that as  $\rho_1$  and  $\rho_2 \Rightarrow 1$ , the intensity remains constant throughout the lifetime.

$F_{R_m}$  for different combination of load parameters are compared in Fig. 6.  $\rho_1 = \rho_2 = \rho$ ,  $t = 20$  yr,  $\mu_{d_1} = \mu_{d_2} = 0.005$  yr,  $\lambda_1 = \lambda_2 = \lambda$ ,  $X^{(1)}$  and  $X^{(2)}$  are normal with  $\mu_{X(1)} = \mu_{X(2)} = 1.0$ ,  $\sigma_{X(1)} = \sigma_{X(2)} = 0.3$ . The rest are indicated in the figure. Monte-Carlo simulation results are shown for the case  $\rho = 0.95$ ; they compared well with analytical solution. Again, it is observed that unless the correlation is almost perfect (i.e.  $\rho = 1.0$ ), the effect of correlation is quite moderate and only significant in the medium range and lower tail of the distribution.

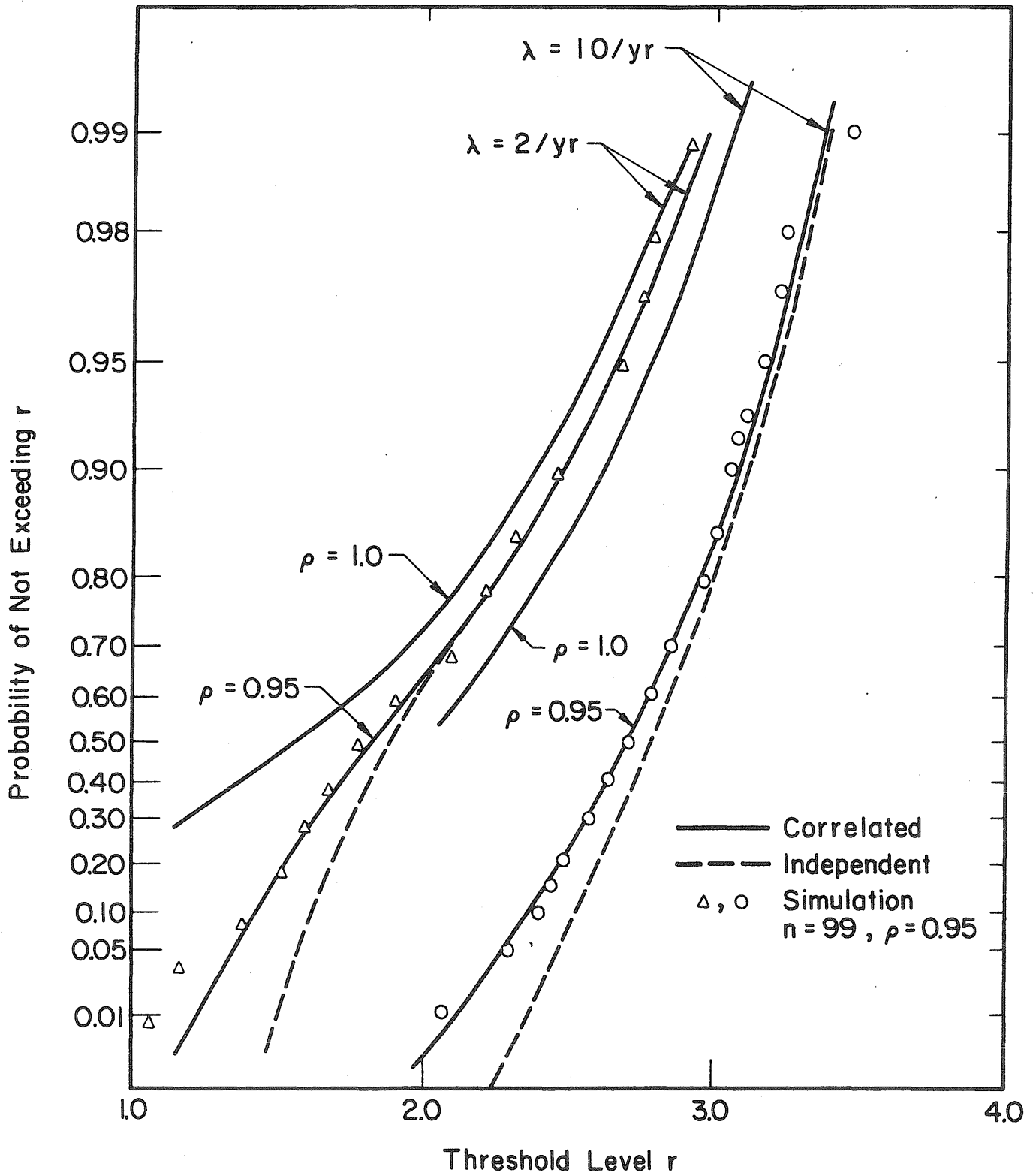


Fig. 6 Effect of Within-Load Intensity Dependence

### III. BETWEEN-LOAD DEPENDENCIES

Loads under combination may be correlated in occurrence time and intensity.

#### 3.1 Occurrence Clustering Among Loads

Examples are extreme wind, wave, snow, rain-on-snow load and loads causing "common-mode" failure in nuclear structures. These loadings may have different arrival times, intensities, but may be clustered around a common point in time that there is a much higher chance of coincidence. Such occurrence clusters are taken into consideration by using a multivariate point process. Individually, the occurrence of each load is a simple Poisson point process, however, collectively, there is a clustering among loads to reflect the physical processes by which these loadings are generated. In Fig. 7 two such correlated processes are described. The parent point process is indicated by a "O", a simple Poisson process with an occurrence rate  $\rho$ . The load may occur (with a probability  $p_i$ ) at a random delay time  $T_i$  and indicated by a " $\Delta$ ". For example, if the parent process represents strong motion earthquakes and the delayed process LOCA loadings, the latter does not always occur after each earthquake and also, the exact time of occurrence may vary. To make the process more general, an independent (noise) Poisson process with occurrence rate  $\rho_i$ , is superimposed and indicated by an "x". The addition of the noise process is to accommodate the situation that the loading can be caused by other sources than the parent process under consideration, e.g. LOCA loadings can be caused by events other than earthquakes such as equipment malfunctions or human errors. " $\Delta$ " and "x" together form the occurrence time for the process  $S_i(t)$  which can be shown (2) to be a simple Poisson process with an occurrence rate  $\lambda_i = \rho_i + \rho p_i$ . The dura-

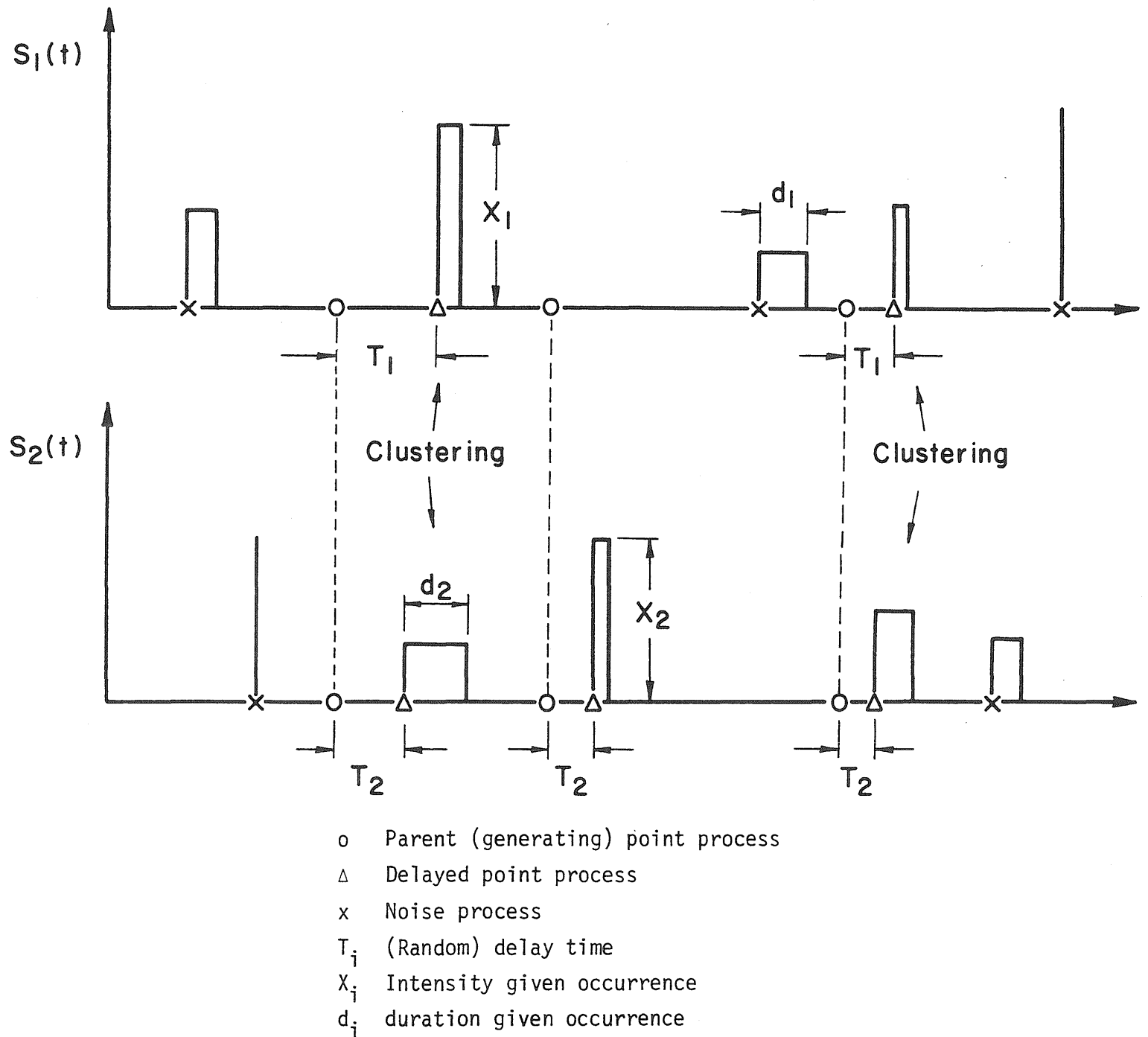


Fig. 7 Definition Sketch

tion and intensity given the occurrence are modeled by random variables such that  $S_i(t)$  is a Poisson renewal pulse process with the mean duration being  $\mu_{d_i}$  and intensity distribution function  $F_{X_i}(x_i)$ . One can make one of  $S_i(t)$  a generating process by setting the delay time equal to zero (it coincides with the parent process) to represent the intensity variation within each occurrence, e.g. local wind storms.

### 3.1.1 Conditional Occurrence Rate Function (COR)

For two correlated processes, the occurrence of one process strongly influences the probability of occurrence of the other. The occurrence correlation of a bivariate point process can be specified in a number of ways. The one that is most convenient for load combination analysis is through the use of conditional occurrence rate (COR) functions defined in the following. (Throughout this paper emphasis is on engineering application rather than mathematical rigor. Readers are referred to Ref. 2 for more rigorous definitions and derivations.)

$$h_1^{(2)}(t) = \lim_{\Delta t \rightarrow 0} \frac{1}{\Delta t} P \{N^{(2)}(t, t+\Delta t) \geq 1 \mid S_1(t) \text{ is "on" at } t=0\} \quad (3.1)$$

in which  $h_1^{(2)}(t)$  = the COR function of  $S_2(t)$  given  $S_1(t)$  is "on" at  $t=0$ ,  $N^{(2)}$  = number of occurrences of  $S_2(t)$ , and  $t=0$  is chosen at the time  $S_1(t)$  is "on". In Ref. 2  $h_1^{(2)}(t)$  is called "cross-intensity." To avoid confusion with the load intensity, COR is used here instead. From Eq. 3.1 one can see that  $h_1^{(2)}(t)$  is similar in concept to the hazard function commonly used in system reliability.  $h_2^{(1)}(t)$  is similarly defined by switching the indices 1 and 2. As  $t \rightarrow \infty$ , the influence of the other process vanishes,  $h_1^{(2)}(t) \Rightarrow \lambda_2$  and  $h_2^{(1)}(t) \Rightarrow \lambda_1$ ; also by definition  $h_1^{(2)}(t)\lambda_1 = h_{(2)}^{(2)}(-t)\lambda_2$  and

$$\lambda_1 h_1^{(2)}(t) = \gamma_1^{(2)}(t) + \lambda_1 \lambda_2 \quad (3.2)$$

in which  $\gamma_1^{(2)}(t)$  is the covariance intensity function

$$\gamma_1^{(2)}(t) = \lim_{\Delta^1 t \rightarrow 0, \Delta^2 t \rightarrow 0} \frac{\text{cov}\{N^{(1)}(0, \Delta^1 t) N^{(2)}(t, t + \Delta^2 t)\}}{\Delta^1 t \Delta^2 t} \quad (3.3)$$

In the above bivariate point process, all points, except the pair generated by the parent process, are statistically independent. The only contribution to  $\gamma_1^{(2)}(t)$  is from this pair. It can be shown

that

$$\gamma_1^{(2)}(t) = P_1 P_2^0 f_{T_2 - T_1}(t) \quad (3.4)$$

in which  $f_{T_2 - T_1}$  = probability density function of the difference of the delay time  $T_2 - T_1$ , therefore (from Eqs. 3.2 and 3.4)

$$h_1^{(2)}(t) = \frac{P_1 P_2^0}{\lambda_1} f_{T_2 - T_1}(t) + \lambda_2 \quad (3.5)$$

$h_2^{(1)}(t)$  is similarly obtained by switching indices 1 and 2. One can obtain a closed form  $f_{T_2 - T_1}$  by using convenient delay time distributions, e.g., one-parameter exponential, Erlang and uniform distribution, two-parameter normal, gamma distribution, etc. The function  $f_{T_2 - T_1}(t)$  for some of the distributions are given in Table 1. The delay times  $T_1$  and  $T_2$  are assumed to be independent; dependence can be introduced by using bivariate distributions. The behavior of  $h_1^{(2)}(t)$  for these delay times is shown in Fig. 8 for  $a_2 = a_1$  and  $a_2 = 2a_1$  where  $a_i = E(T_i)$ . The strong dependence of  $S_2(t)$  on  $S_1(t)$  can be seen by the sharp increase as  $|t| \rightarrow 0$ , however, this dependence vanishes (independent) as  $|t| \rightarrow \infty$ ; also, when parameters being comparable  $h_1^{(2)}(t)$  is not particularly sensitive to the distribution type.

TABLE 1 Function  $f_{T_2 - T_1}(\tau)$ 

Delay Time Distribution	$f_{T_2 - T_1}(\tau)$
Exponential $E(T_1) = a_1$ $E(T_2) = a_2$ (C.O.V. $\delta_{T_i} = 1$ )	$\frac{1}{a_1 + a_2} e^{-\tau/a_2} \quad \text{for } \tau > 0$ $\frac{1}{a_1 + a_2} e^{\tau/a_1} \quad \text{for } \tau < 0$
Erlang $E(T_1) = a_1$ $E(T_2) = a_2$ (C.O.V. $\delta_{T_i} = .707$ )	$\frac{4e^{-2\tau/a_2}}{(a_1 + a_2)^2} \left[ \tau + \frac{a_1 a_2}{(a_1 + a_2)} \right] \quad \text{for } \tau > 0$ $\frac{4e^{2\tau/a_1}}{(a_1 + a_2)^2} \left[ \tau + \frac{a_1 a_2}{(a_1 + a_2)} \right] \quad \text{for } \tau < 0$
Uniform $E(T_1) = a_1$ $E(T_2) = a_2$ ( $\delta_{T_i} = .577$ )	$\frac{2a_2 + \tau}{4a_1 a_2} \quad \text{for } a_2 > a_1 \text{ and } -2a_1 < \tau < 0$ $\frac{1}{2a_2} \quad \text{for } 0 < \tau < 2(a_2 - a_1)$ $\frac{2a_2 - \tau}{4a_1 a_2} \quad \text{for } 2(a_2 - a_1) < \tau < 2a_2$ $0 \quad \text{otherwise}$ <p>for <math>a_1 &gt; a_2</math> switch indices 1 &amp; 2</p>
Normal $E(T_1) = a_1$ $E(T_2) = a_2$ $\sigma_{T_1}, \sigma_{T_2}$ Standard Deviation	$\frac{1}{\sqrt{2\pi} \sqrt{\sigma_{T_1}^2 + \sigma_{T_2}^2}} \exp\left[-\frac{1}{2} \frac{[\tau - (a_2 - a_1)]^2}{\sigma_{T_1}^2 + \sigma_{T_2}^2}\right]$

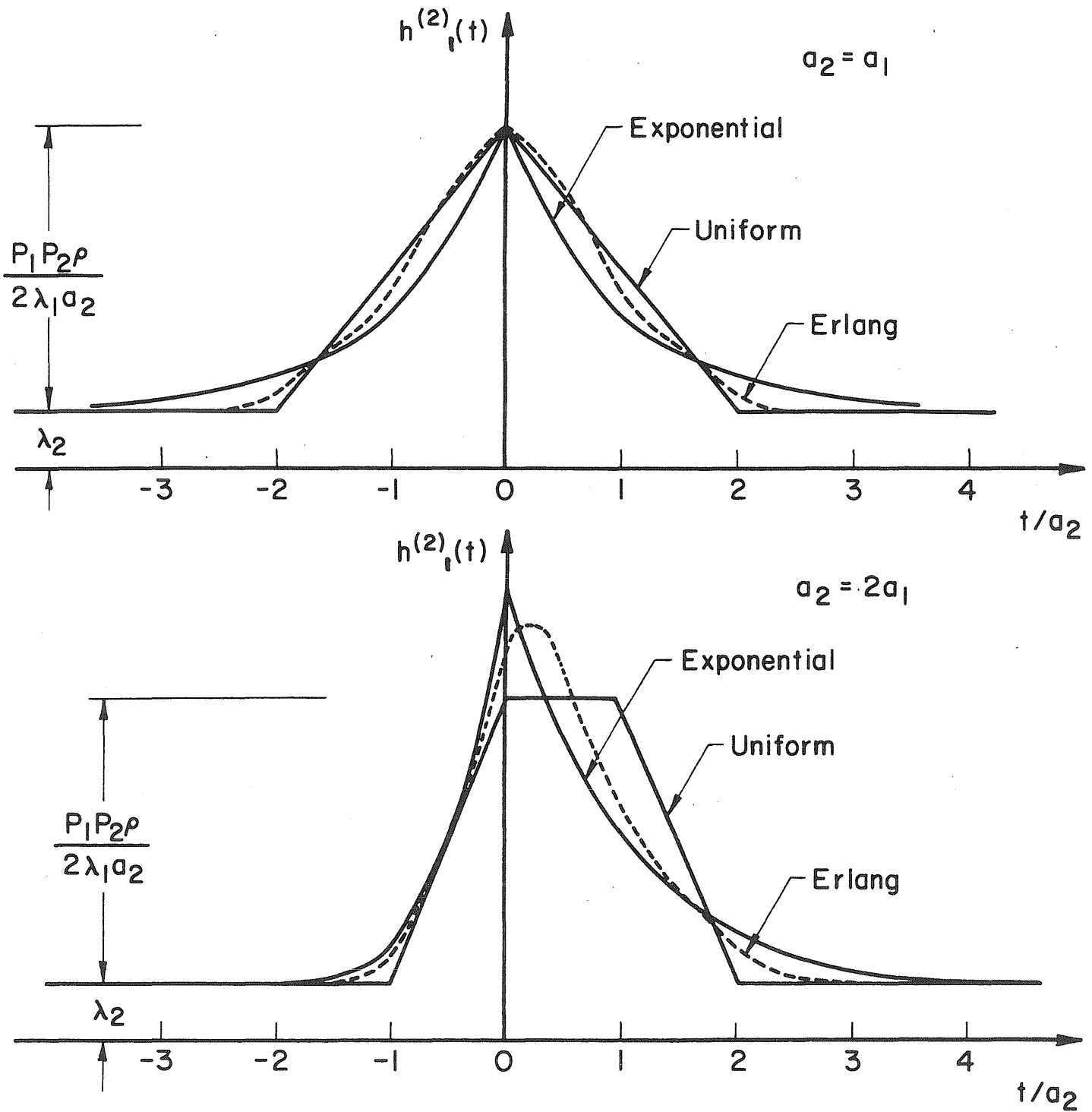


Fig. 8 Conditional Occurrence Rate (C.O.R.) Function



The dependence on distribution parameters should be obvious, i.e. the peak shifts with  $E(T_2) - E(T_1)$  and the concentration is governed by  $\sqrt{\sigma_{T_1}^2 + \sigma_{T_2}^2}$ . Alternatively, if information is available on the delay time difference  $T_2 - T_1$ , one can use such information directly without having first to model individual delay times.

### 3.1.2 Two-Load Coincidence Rate Analysis

Coincidence of processes  $S_1(t)$  and  $S_2(t)$  can happen in two mutually exclusive ways, i.e.  $S_1(t)$  is "on" at  $t = \tau$  and  $S_2(t)$  is "on" in  $(\tau, \tau + d_1)$ , or  $S_2(t)$  is "on" at  $t = \tau$  and  $S_1(t)$  is "on" in  $(\tau, \tau + d_2)$  in which  $d_1$  and  $d_2$  are the durations of the two processes given occurrences. Therefore

$$\begin{aligned}
 & P(\text{coincidence} \mid d_1, d_2) \\
 &= P [N^{(2)}(\tau, \tau + d_1) \geq 1 \mid S_1(t) \text{ is "on" in } \tau, \tau + \Delta t] \\
 & \quad P [S_1(t) \text{ is "on" in } \tau, \tau + \Delta t] + P [N^{(1)}(\tau, \tau + d_2) \geq 1 \mid S_2(t) \text{ is "on" in} \\
 & \quad \tau, \tau + \Delta t] \geq 1] \quad P [S_2(t) \text{ is "on" in } \tau, \tau + \Delta t] \\
 &= g_2(d_1) \lambda_1 \Delta t + g_1(d_2) \lambda_2 \Delta t \tag{3.6}
 \end{aligned}$$

in which  $g_2$  and  $g_1$  indicate the conditional probabilities. Taking expectation with respect to  $d_1$  and  $d_2$ , dividing by  $\Delta t$  and letting  $\Delta t \rightarrow 0$ , one obtains the mean rate of coincidence

$$\lambda_{12} = \lim_{\Delta t \rightarrow 0} \frac{P}{\Delta t} = E_d [g_2(d_1) \lambda_1 + E_d [g_1(d_2)] \lambda_2] \tag{3.7}$$

in which  $E_d [ \ ]$  = expectation W.R.T. durations. A convenient first-order approximation is

$$\lambda_{12} \approx g_2(\mu_{d_1}) \lambda_1 + g_1(\mu_{d_2}) \lambda_2 \tag{3.8}$$

in which  $\mu_{d_1}$ ,  $\mu_{d_2}$  are the mean load durations.

Using the COR function, one can show that

$$\begin{aligned}
g_2(x) &= P[N^{(2)}(\tau, \tau+x) \geq 1 \mid S_1(t) \text{ is "on" at } \tau] \\
&= 1 - \exp\left[-\int_0^x h_1^{(2)}(\tau) d\tau\right]
\end{aligned} \tag{3.9}$$

The function  $g_2$  for the COR functions given in Table 1 are obtained in closed form and given in Table 2.  $g_1$  can be similarly obtained. Approximations for  $g_2$  under the condition that load durations are small, i.e.  $\lambda_2 \mu_{d_1} \ll 1$  and  $\mu_{d_1}/a_2 \ll 1$  are also indicated by  $\hat{g}_2$  in Table 2. To check the accuracies of the approximations in Eq. 3.8 and Table 2.  $E_d[g_2]$  is evaluated numerically in which an exponential distribution is used for  $d_1$  (since the process is a Poisson renewal pulse process). Comparison of results (see Table 3) indicates that Eq. 3.8 is generally satisfactory, and  $\hat{g}_2$  in Table 2 is satisfactory for small  $\mu_{d_1}$  and can be used at least as an order-of-magnitude type of estimate for large  $\mu_{d_1}$ . Also, the results are not very sensitive to the delay time distribution. The same is true of course for  $g_1$ . For example, if the delay times can be modeled by exponential distributions and the durations are small, from Eq. 3.8 and the approximations  $\hat{g}_1$  and  $\hat{g}_2$  for  $g_1$  and  $g_2$  one obtains the coincidence rate

$$\lambda_{12} \approx \lambda_1 \lambda_2 (\mu_{d_1} + \mu_{d_2}) \left[ 1 + \frac{p_1 p_2}{\lambda_1 \lambda_2} \frac{1}{(a_1 + a_2)} \right] \tag{3.10}$$

If  $p_1$  or  $p_2 = 0$ , i.e. at least one of the two load processes is not generated by the parent process, namely, the clustering no longer exists and  $S_1(t)$  and  $S_2(t)$  are statistically independent, Eq. 3.10 reduces to the result previously obtained (6).

TABLE 2 Function  $g_2(\mu_{d_1})$

Distribution (see Table 1)	$g_2(\mu_{d_1})$	$\hat{g}_2(\mu_{d_1})$
Exponential	$1 - \exp[-\lambda_2 \mu_{d_1} - \frac{P_1 P_2 \rho}{\lambda_1} (\frac{a_2}{a_1 + a_2}) (1 - e^{-\mu_{d_1}/a_2})]$	$[\lambda_2 + \frac{P_1 P_2 \rho}{\lambda_1} \frac{1}{(a_1 + a_2)}] \mu_{d_1}$
Erlang	$1 - \exp\{-\lambda_2 \mu_{d_1} - \frac{P_1 P_2 \rho}{\lambda_1 (a_1 + a_2)^2} [a_2^2 (1 - e^{-2\mu_{d_1}/a_2}) + \frac{2a_2}{(1/a_1 + 1/a_2)} (1 - e^{-2\mu_{d_1}/a_2}) - 2a_2 \mu_{d_1} e^{-2\mu_{d_1}/a_2}]\}$	$[\lambda_2 + \frac{4P_1 P_2 \rho}{\lambda_1} \frac{a_1 a_2}{(a_1 + a_2)^3}] \mu_{d_1}$
Normal	$1 - \exp\{-\lambda_2 \mu_{d_1} - \frac{P_1 P_2 \rho}{\lambda_1} [\phi(\frac{\mu_{d_1} - (a_2 - a_1)}{\sqrt{\sigma_1^2 + \sigma_2^2}}) - \phi(\frac{a_1 - a_2}{\sqrt{\sigma_1^2 + \sigma_2^2}})]\}$	$[\lambda_2 + \frac{P_1 P_2 \rho}{\sqrt{2\pi(\sigma_1^2 + \sigma_2^2)}} e^{-1/2 \frac{(a_2 - a_1)^2}{\sigma_1^2 + \sigma_2^2}}] \mu_{d_1}$
Uniform	for $a_2 > a_1$ (switch the indices 1 and 2 for $a_2 < a_1$ ) $1 - \exp\{-\lambda_2 \mu_{d_1} - \frac{P_1 P_2 \rho}{2\lambda_1 a_2} \mu_{d_1}\}$ for $\mu_{d_1} \leq 2(a_2 - a_1)$ $1 - \exp\{-\lambda_2 \mu_{d_1} - \frac{P_1 P_2 \rho}{\lambda_1} (1 - a_1/2a_2)\}$ for $\mu_{d_1} > 2a_2$ $1 - \exp\{-\lambda_2 \mu_{d_1} - \frac{P_1 P_2 \rho}{\lambda_1} [(1 - a_1/a_2) + 1/4(1/a_2 + \frac{2a_2 - \mu_{d_1}}{2a_1 a_2}) (\mu_{d_1} - 2a_2 + 2a_1)]\}$ otherwise	$[\lambda_2 + \frac{P_1 P_2 \rho}{2\lambda_1 a_2}] \mu_{d_1}$

TABLE 3 Comparison of  $g_2(\nu_{d_1})$ ,  $\hat{g}_2(\nu_{d_1})$   
with  $E[g_2(d_1)]$

$\frac{a_2}{a_1}$	Dist.	Func.	$\nu_{d_1} / a_2$			
			.1	.5	1.0	5.0
1	Exp.	$E[g_2]$	.920-2	.334-1	.501-1	.882-1
		$g_2$	.966-2	.395-1	.631-1	.103
		$\hat{g}_2$	.102-1	.510-1	.102	.510
	Erlang	$E[g_2]$	.981-2	.373-1	.553-1	.913-1
		$g_2$	.100-1	.447-1	.721-1	.104
		$\hat{g}_2$	.102-1	.510-1	.102	.510
	Uniform	$E[g_2]$	.959-2	.375-1	.564-1	.924-1
		$g_2$	.990-2	.437-1	.741-1	.104
		$\hat{g}_2$	.102-1	.510-1	.102	.510
5	Exp.	$E[g_2]$	.345-2	.158-1	.289-1	.874-1
		$g_2$	.349-2	.167-1	.316-1	.108
		$\hat{g}_2$	.353-2	.176-1	.353-1	.176
	Erlang	$E[g_2]$	.217-2	.123-1	.258-1	.952-1
		$g_2$	.212-2	.117-1	.254-1	.124
		$\hat{g}_2$	.205-2	.103-1	.205-1	.103
	Uniform	$E[g_2]$	.219-2	.108-1	.214-1	.868-1
		$g_2$	.219-2	.109-1	.217-1	.104
		$\hat{g}_2$	.220-2	.110-1	.220-1	.110

$$\lambda_1 = \lambda_2 = 2, P_1 = P_2 = 1$$

To examine the sensitivity of increase in coincidence rate to the clustering, consider the combination of two load processes in which  $\rho_1 = \rho_2 = 0$  (no noise processes),  $\lambda_1 = \lambda_2 = \rho = 1/\text{yr}$ , mean delay times  $a_1 = a_2 = 10^{-3}$  yr ( 8 hrs.), mean durations  $\mu_{d_1} = \mu_{d_2} = 10^{-4}$  yr ( 50 min.) and  $p_1 = p_2 = 1$  (the loadings always occur after the parent process). An independence assumption would give a coincidence rate of  $2 \times 10^{-4}/\text{yr}$ , while after including clustering effect, it increases to (from Eq. 3.10)  $10^{-1}/\text{yr}$ , a factor of  $5 \times 10^2$ . Of course, in this case the fact that the mean delay times are equal and the uncertainties (coefficient of variation  $\delta_{T_1} = \delta_{T_2} = 1.0$ ) are large also contribute to the high coincidence rate. If  $a_1 \neq a_2$  and  $\delta_{T_1}$  and  $\delta_{T_2}$  are much smaller, the coincidence rate would be reduced somewhat. For example, if  $a_1 = 10^{-3}$  yr,  $a_2 = 2.0 \times 10^{-3}$  yr,  $\delta_{T_1} = \delta_{T_2} = 0.3$  and all other parameters remain the same, assuming the delay times to be normal, from Eq. 3.8 and Table 2 one obtains a coincidence rate of  $3.9 \times 10^{-2}/\text{yr}$ .

### 3.1.3 Occurrence Dependence Among Three Loads

The above method of modeling and analysis can be extended to the case of combination of more than two loads. Generally speaking, there may be more than one parent process and different ways of clustering which may require different treatments. Consider the simple case of combination of three loads with possible clustering around a common parent point process by adding one more Poisson renewal pulse process to the foregoing two-load model. It consists of a clustering part (with delay time  $T_3$ , probability of being "on" given the occurrence of the parent

process  $P_3$ ) and a noise part (with occurrence rate  $\rho_3$ ). The mean duration =  $\mu_{d_3}$  and intensity distribution =  $F_{X_3}(x_3)$ . The analysis of correlation and coincidence rate between any two load processes is no different from that in the preceding sections. However, when all three loads are considered, the dependence of one load process on the occurrences of the other two needs to be taken into consideration. For this purpose, a two-time COR function is defined as follows:

$$h_{12}^{(3)}(t, t') = \lim_{\Delta t \rightarrow 0} \frac{1}{\Delta t} P[N^{(3)}(t, t+\Delta t) \geq 1 \mid S_1(t) \text{ is "on" at } t=0$$

$$\text{and } S_2(t) \text{ is "on" at } t=t'] \quad (3.11)$$

in which  $t=0$  is chosen at the time  $S_1(t)$  is "on";  $h_{12}^{(3)}$  is the conditional occurrence rate of  $S_3(t)$ , those of  $S_1(t)$ ,  $h_{23}^{(1)}$ , and  $S_2(t)$ ,  $h_{13}^{(2)}$  are similarly defined. Some asymptotic properties of the function  $h_{12}^{(3)}(t, t')$  are as follows: as  $|t|$ , and  $|t-t'| \Rightarrow \infty$ ,  $S_3(t)$  would be free of the influence of  $S_1(t)$  and  $S_2(t)$ , therefore  $h_{12}^{(3)} = \lambda_3$ ; also as  $|t| \Rightarrow \infty$  but  $|t-t'|$  remains finite,  $S_3(t)$  would be dependent only on  $S_2(t)$ , therefore,  $h_{12}^{(3)} = h_2^{(3)}$ . Following a procedure similar to that for the two-load case one can show that (derivation given in Appendix B)

$$h_{12}^{(3)}(t, t') = \frac{\gamma_{123}(t, t')}{\lambda_1 h_1^{(2)}(t')} + \frac{\lambda_2}{h_1^{(2)}(t')} [h_2^{(3)}(t-t') + h_1^{(3)}(t') - 2\lambda_3] + \lambda_3 \quad (3.12)$$

$$\text{in which } \gamma_{123}(t, t') = \rho \rho_1 \rho_2 \rho_3 \int_0^{\infty} f_{T_2}(t'+\tau) f_{T_3}(t+\tau) f_{T_1}(\tau) d\tau$$

and the delay times  $T_1$ ,  $T_2$  and  $T_3$  are assumed to be independent. For example, if the delay times follow exponential distributions it can be shown

$$\begin{aligned}
h_{12}^{(3)}(t, t') = & \frac{1}{\left[ \frac{\lambda_1 \lambda_2}{\rho} + \frac{p_1 p_2}{(a_1 + a_2)} e^{-t'/a_2} \right]} \left\{ \frac{p_1 p_2 p_3}{(a_1 a_2 + a_2 a_3 + a_1 a_3)} e^{-(t'/a_2 + t/a_3)} \right. \\
& \left. + \frac{\lambda_1 p_2 p_3}{(a_2 + a_3)} e^{-(t-t')/a_3} + \frac{\lambda_2 p_1 p_3}{(a_1 + a_3)} e^{-t/a_3} \right\} + \lambda_3 \quad \text{for } t > t' \quad (3.13)
\end{aligned}$$

and for  $t < t'$ ,  $-(t't')/a_3$  in Eq. 3.13 is replaced by  $(t-t')/a_2$ . Similarly, one can obtain  $h_{23}^{(1)}$  and  $h_{13}^{(2)}$  by rotating the indices. Note also, that Eq. 3.13 satisfies all the asymptotic properties required for the two-time COR function. The behavior of the conditional occurrence rate function of  $S_3(t)$ ,  $h_{12}^{(3)}$ , is shown in Fig. 9 for the case  $p_1 = p_2 = p_3 = 1$ ,  $a_1 = a_2 = a_3 = a$  (equal mean delay times) and  $\rho_1 = \rho_2 = \rho_3 = 0$  (no noise processes). The surface described by the two-time COR function is a two-dimensional version of the one-time COR function. The sharp ridge at  $t = t'$  indicates the strong influence of the occurrence of  $S_2(t)$ , even when  $t$  is large (i.e. influence of  $S_1(t)$  already vanishes). The maximum is at  $t = t' = 0$ , the time when both  $S_1(t)$  and  $S_2(t)$  are "on". Different delay time distributions may cause slightly different behavior, for example if all three delay times are modeled by Erlang distributions, the surface would be similar except the ridge would be smooth.

#### 3.1.4 Three-Load Coincidence Rate Analysis

Coincidence of three loads can occur in  $3! = 6$  mutually exclusive ways according to the order of the "on" times of the three processes. For example (see Fig. 10), if processes  $S_1(t)$ ,  $S_2(t)$ , and  $S_3(t)$  are "on" according to the order 1, 2 and 3 and  $S_1(t)$  is "on" at  $t = t_0$ , then coincidence of three levels occurs if  $S_2(t)$  is "on" at  $t = t'$ , where

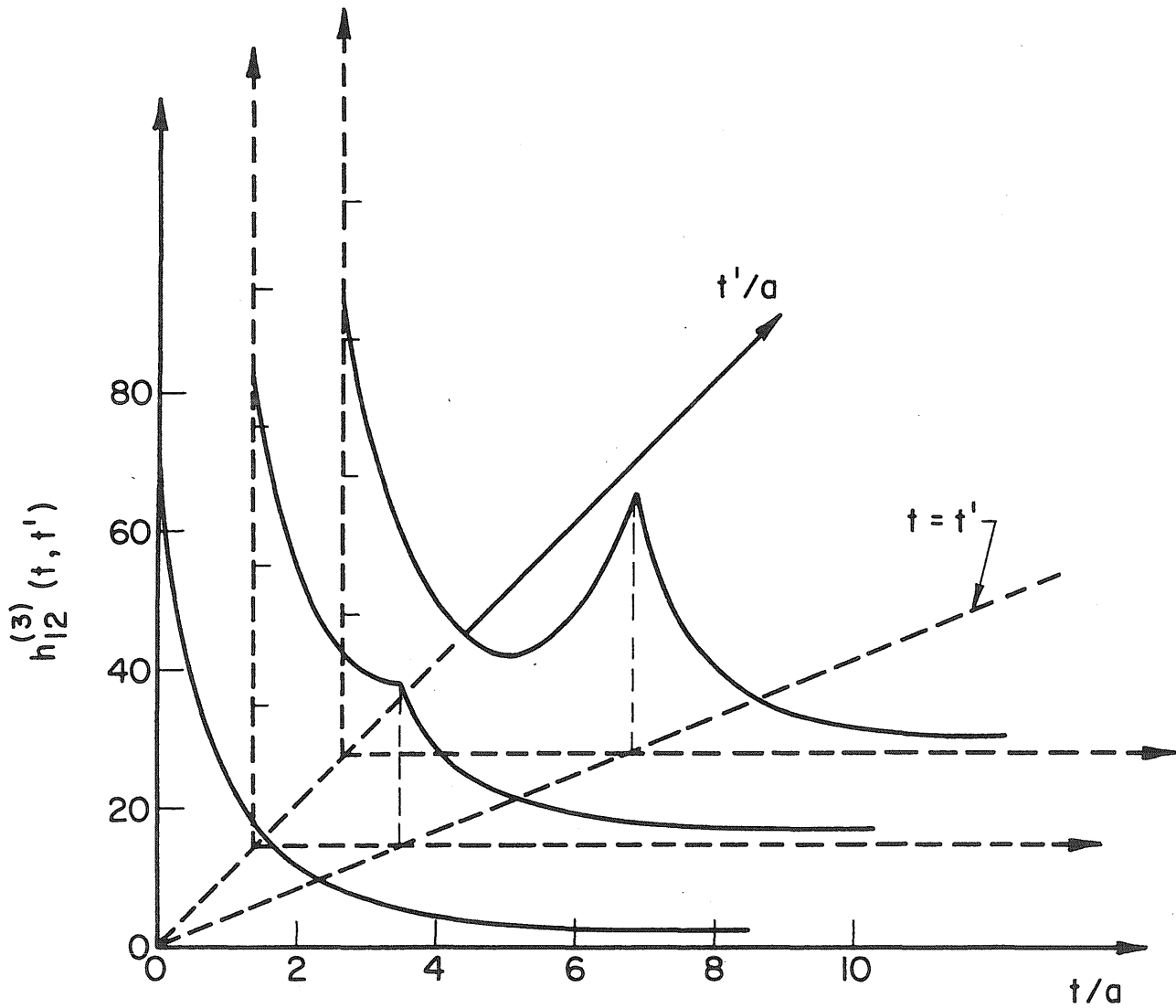


Fig. 9 Two-Time C.O.R. Function  $h_{12}^{(3)}(t, t')$   
 $(\rho = 2 / \text{yr}, a = 10^{-2} \text{ yr})$



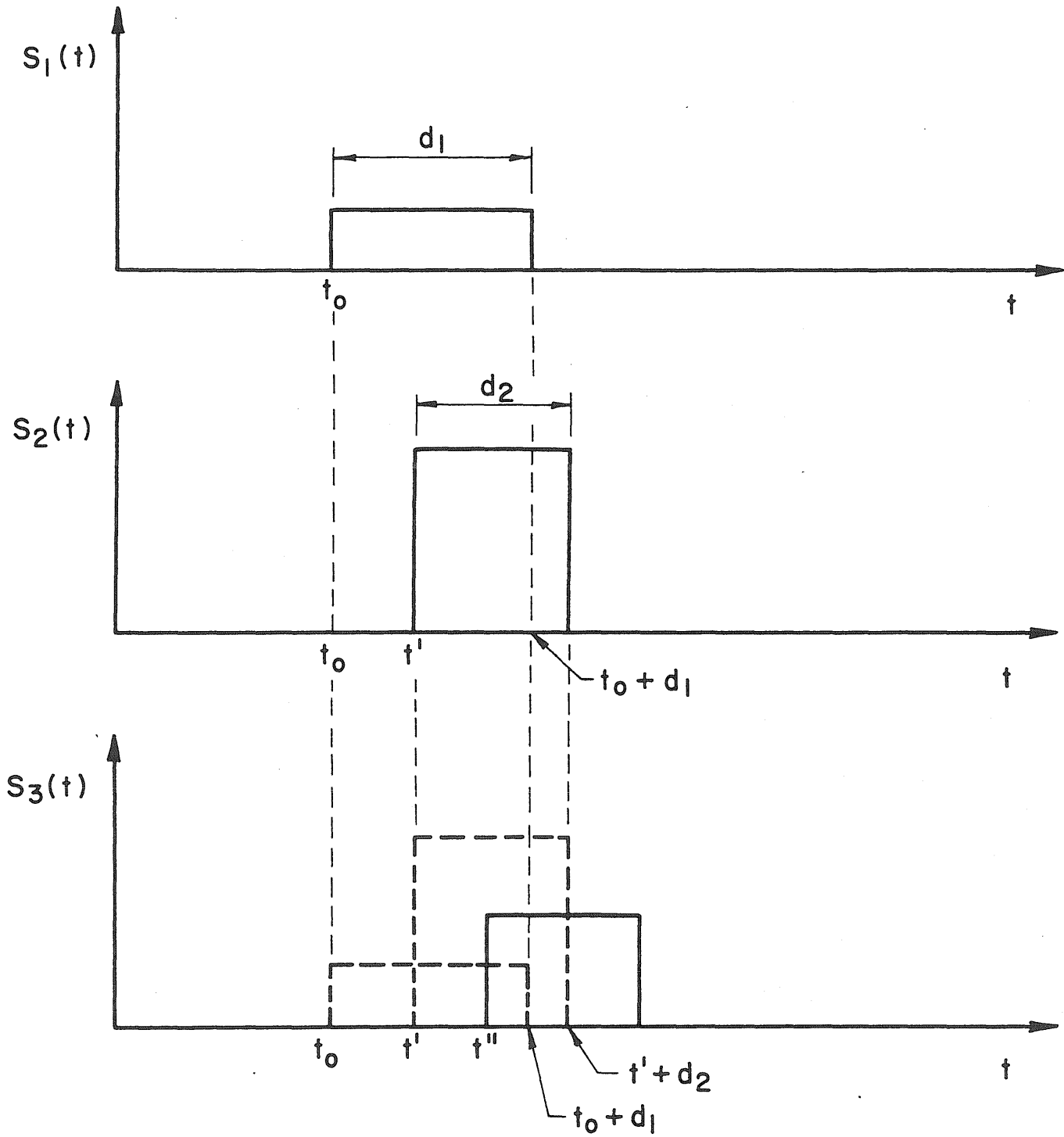


Fig. 10 Coincidence of Three Loads

$t_0 < t' < t_0 + d_1$  and  $S_3(t)$  is "on" at  $t=t'$ , where  $t' < t' < \min(t_0 + d_1, t' + d_2)$ .

Following a procedure similar to that given in Eqs. 3.6 and 3.7, it can be shown that contribution to the coincidence rate from this occurrence sequence is

$$\lambda_1 E_d[g_{123}(d_1, d_2)] \approx \lambda_1 g_{123}(\mu_{d_1}, \mu_{d_2}) \quad (3.14)$$

in which  $g_{123}(d_1, d_2)$  is the conditional probability that  $S_2(t)$  and  $S_3(t)$  are "on" according to the manner described above given the durations of  $S_1(t)$  and  $S_2(t)$  being  $d_1$  and  $d_2$  and that  $S_1(t)$  has occurred.  $E_d[ ]$  is the expectation w.r.t. the durations for which a first-order approximation can be used. Using the conditional occurrence rate functions, the mean number of joint occurrences of  $S_2(t)$  and  $S_3(t)$  in the time intervals as described is

$$\mu_{23} = \int_0^{d_1} h_1^{(2)}(t') \int_{t'}^{\min(d_1, t'+d_2)} h_{12}^{(3)}(t, t') dt dt' \quad (3.15)$$

in which  $S_1(t)$  is assumed to be "on" at  $t=0$ . Therefore,

$$\begin{aligned} g_{123}(d_1, d_2) &\approx 1 - \exp[-\mu_{23}] \\ &\approx \mu_{23} \quad \text{for } \mu_{23} \ll 1 \end{aligned} \quad (3.16)$$

Similarly  $g_{ijk}$  for other sequence of occurrence of the loads can be obtained by rotating indices in Eqs. 3.15 and 3.16.

The overall coincidence rate regardless of the order of "on" times is therefore the sum (since they are mutually exclusive) given by

$$\begin{aligned} \lambda_{123} &\approx \lambda_1 E_d[g_{123}(d_1, d_2) + g_{132}(d_1, d_3)] + \lambda_2 E_d[g_{213}(d_2, d_1) + \\ &g_{231}(d_2, d_3)] + \lambda_3 E_d[g_{312}(d_3, d_1) + g_{321}(d_3, d_2)] \end{aligned} \quad (3.17)$$

in which approximations given by Eqs. 3.14 and 3.16 can be used. Integration in Eq. 3.15 can be carried out in closed form for some delay time distributions (see Appendix C). A further approximation can be used when the load durations are small, i.e.  $\mu_{d_i}/a_j \ll 1$  and  $\lambda_i \mu_{d_j} \ll 1$ ,

$$g_{123}(d_1, d_2) \approx \hat{g}_{123} = h_1^{(2)}(0) h_{12}^{(3)}(0,0) \int_0^{d_1} \int_{t'}^{\min(d_1, t'+d_2)} dt dt'$$

$$= \begin{cases} h_1^{(2)}(0) h_{12}^{(3)}(0,0) d_1^2/2 & \text{for } d_1 \leq d_2 \\ h_1^{(2)}(0) h_{12}^{(3)}(0,0) [d_1 d_2 - d_2^2/2] & \text{for } d_1 > d_2 \end{cases} \quad (3.18)$$

in which, for example, if delay times are exponential variates, from Eqs. 3.13, 3.5, and Table 1

$$h_1^{(2)}(0) h_{12}^{(3)}(0,0) = \frac{\rho}{\lambda_1} \left[ \frac{p_1 p_2 p_3}{(a_1 a_2 + a_2 a_3 + a_1 a_3)} + \frac{\lambda_1 p_2 p_3}{(a_2 + a_3)} + \frac{\lambda_2 p_1 p_3}{(a_1 + a_3)} + \frac{\lambda_3 p_1 p_2}{(a_1 + a_2)} \right] + \lambda_2 \lambda_3 \quad (3.19)$$

An interesting limiting case is when at least two among the three  $P_i$ 's are zero, i.e. the clustering around the parent process no longer exists and  $S_1(t)$ ,  $S_2(t)$ , and  $S_3(t)$  become statistically independent. Substituting Eqs. 3.18 and 3.19 into Eq. 3.17, knowing that for this case  $h_1^{(2)}(0) h_{12}^{(3)}(0,0) = \lambda_2 \lambda_3$ , etc. one obtains

$$\lambda_{123} \approx \lambda_1 \lambda_2 \lambda_3 (\mu_{d_1} \mu_{d_2} + \mu_{d_2} \mu_{d_3} + \mu_{d_1} \mu_{d_3}) \quad (3.20)$$

the result previously obtained (11).

The accuracies of the approximations in Eqs. 3.14 and 3.18 are examined by comparison of results with  $E_d[g_{123}]$  from numerical integration in which the duration distributions are exponential. The results are shown in Table 4. It is seen that  $g_{123}(\mu_{d_1}, \mu_{d_2})$  is generally satisfactory and so is  $\hat{g}_{123}$  for small durations.

The increase in the coincidence rate due to clustering is examined by the following numerical example.  $P_1 = P_2 = P_3 = 1$ ,  $a_1 = a_2 = a_3 = a = 10^{-3}$  ( $\approx 8$  hrs.) and  $\rho_1 = \rho_2 = \rho_3 = 0$  (no noise processes),  $\rho = 1/\text{yr.}$ , and  $\mu_{d_1} = \mu_{d_2} = \mu_{d_3} = \mu_d = 10^{-4}$  ( $\approx 50$  min.). An independence assumption would give (from Eq. 3.20) a coincidence rate of  $\lambda_{123} \approx 3 \times 10^{-8}/\text{yr.}$ , whereas including clustering one obtains from Eqs. 3.17, 3.18, and 3.19

$$\lambda_{123} \approx 3\rho \mu_d^2 \left[ \frac{3\rho}{2a} + \frac{1}{3a^2} \right] + 3\rho^3 \mu_d^2 = 10^{-2}/\text{yr} \quad (3.21)$$

an increase by a factor of  $3.3 \times 10^5$ .

Theoretically, the method can be extended to the analysis of four or more loadings. However, as can be seen the C.O.R. function and the algebra required for the evaluation of the coincidence rate would become extremely complicated, therefore it is not pursued any further in this study.

### 3.1.5 Probability of Lifetime Maximum and Comparison with Simulation Results

The probability distribution function of the lifetime combined maximum of the sum of such clustering processes is (from Eq. 1.1),

$$F_{R_m}(r, T) \approx \exp \left[ - \sum_i \lambda_i T F_{X_i}^*(r) - \sum_{i \neq j} \lambda_{ij} T F_{X_{ij}}^*(r) - \sum_{i \neq j \neq k} \lambda_{ijk} T F_{X_{ijk}}^*(r) \dots \right] \quad (3.22)$$

TABLE 4

Comparison of  $g_{123}$ ,  $\hat{g}_{123}$  with  $E[G_{123}]$ 

	$\mu_{d_1}$	$E[g_{123}]$	$g_{123}$	$\hat{g}_{123}$
$\mu_{d_1}/\mu_{d_2}=1$	.0001	.00133	.00152	.00168
	.0005	.0165	.0257	.0420
	.001	.0364	.0653	.168
	.005	.106	.159	4.2
$\mu_{d_1}/\mu_{d_2}=3$	.0003	.00438	.00628	.00841
	.0015	.0337	.0594	.2102
	.003	.0603	.102	.840
	.015	.131	.169	21.0

$$P_1 = P_2 = P_3 = 1, \rho = 2.0, a_1 = a_2 = a_3 = 0.001$$

$$\rho_1 = \rho_2 = \rho_3 = 0$$

in which  $\lambda_{ij}$  and  $\lambda_{ijk}$  are the coincidence rates given by Eqs. 3.7 and 3.17;  $X_{ij} = X_i + X_j$ ,  $X_{ijk} = X_i + X_j + X_k$ , etc.

In the above approximation the clustering effect on the individual load contribution is neglected since in Section 2.2 it has been shown that such an effect is quite moderate and tends to give lower value of  $R_m$ .

To demonstrate the validity of the proposed method, Monte-Carlo simulations are carried out to verify the accuracies of (1) coincidence rates as given by Eqs. 3.7 and 3.17 and (2) the probability of combined maximum as given by Eq. 3.22. Three load processes with possible clustering as previously described are generated by digital computer.

Sample statistics and probability estimates based on a sample size of  $n=100$  are computed and compared with the theoretical values. According to the analysis the coincidences of loads are Poisson processes with mean rates given by Eqs. 3.7 and 3.17. The comparisons of the coincidence rates for two sets of process parameters are shown in Table 5 (column 1, 2, 6 and 7). The slight difference can be attributed to sampling errors (due to finite sample size). The goodness-of-fit tests of the Poisson distribution are also satisfactory and the results are shown in Table 5.

$F_{R_m}(r, T)$  given by Eq. 3.22 is compared with simulation results in Figs. 11 and 12. Load intensities given occurrence are assumed to be independent normal variates with  $\mu_{x_1} = \mu_{x_2} = \mu_{x_3} = 1.0$ ,  $\sigma_{x_1} = \sigma_{x_2} = \sigma_{x_3} = 0.3$ . The other parameters remain the same as given in Table 5. As expected, at high threshold (low risk) levels, Eq. 3.22 gives very good estimates since the distribution is dominated by the coincidence terms; at low level the Poisson assumption used causes slightly conservative results. Results based on an assumption that the loading occurrences are independent are also shown by dashed lines. As expected, such assumption lead to quite serious underestimates of the risk of combination of loadings.

TABLE 5 Coincidence Statistics

	Two-Load Coincidence					Three-Load Coincidence				
	$\lambda_{12}$		$\chi^2$ test			$\lambda_{123}$		$\chi^2$ test		
	(1) Theory	(2) Simula- tion	(3) Sample $\chi^2$	(4) 5% Signif. $\chi^2$	(5) Most Likely $\chi^2$	(6) Theory	(7) Simula- tion	(8) Sample $\chi^2$	(9) 5% Signif. $\chi^2$	(10) Most Likely $\chi^2$
$P_1=P_2=P_3=1$ $\rho_1=\rho_2=\rho_3=0$	.890	.895	10.85	22.4	11.0	.210	.187	8.80	14.6	4.0
$P_1=P_2=P_3=.5$ $\rho_1=\rho_2=\rho_3=2/\text{yr}$	.352	.351	5.66	14.1	6.0	.0412	.0474	2.86	5.99	1.0

$\mu_{d_1}=\mu_{d_2}=\mu_{d_3} = .005 \text{ yr}$ ,  $a_1=a_2=a_3 = .02 \text{ yr}$ ,  $\rho = 4/\text{yr}$ ,  $T = 20 \text{ yrs}$ , Sample Size  $n=100$

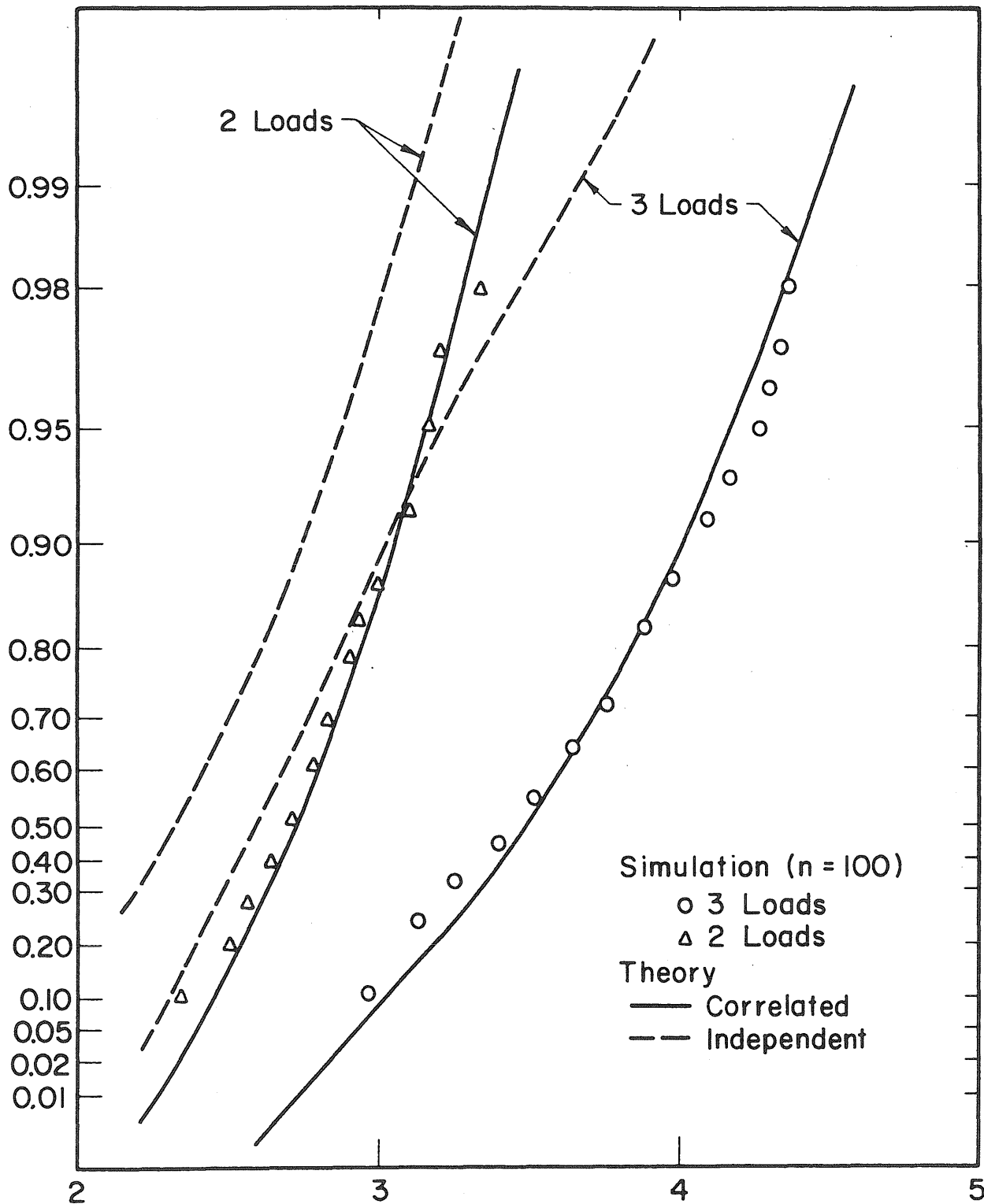


Fig. 11 Probability of Lifetime Combined Maximum  
 $(P_1=P_2=P_3=1, \rho_1=\rho_2=\rho_3=0, \rho=4)$



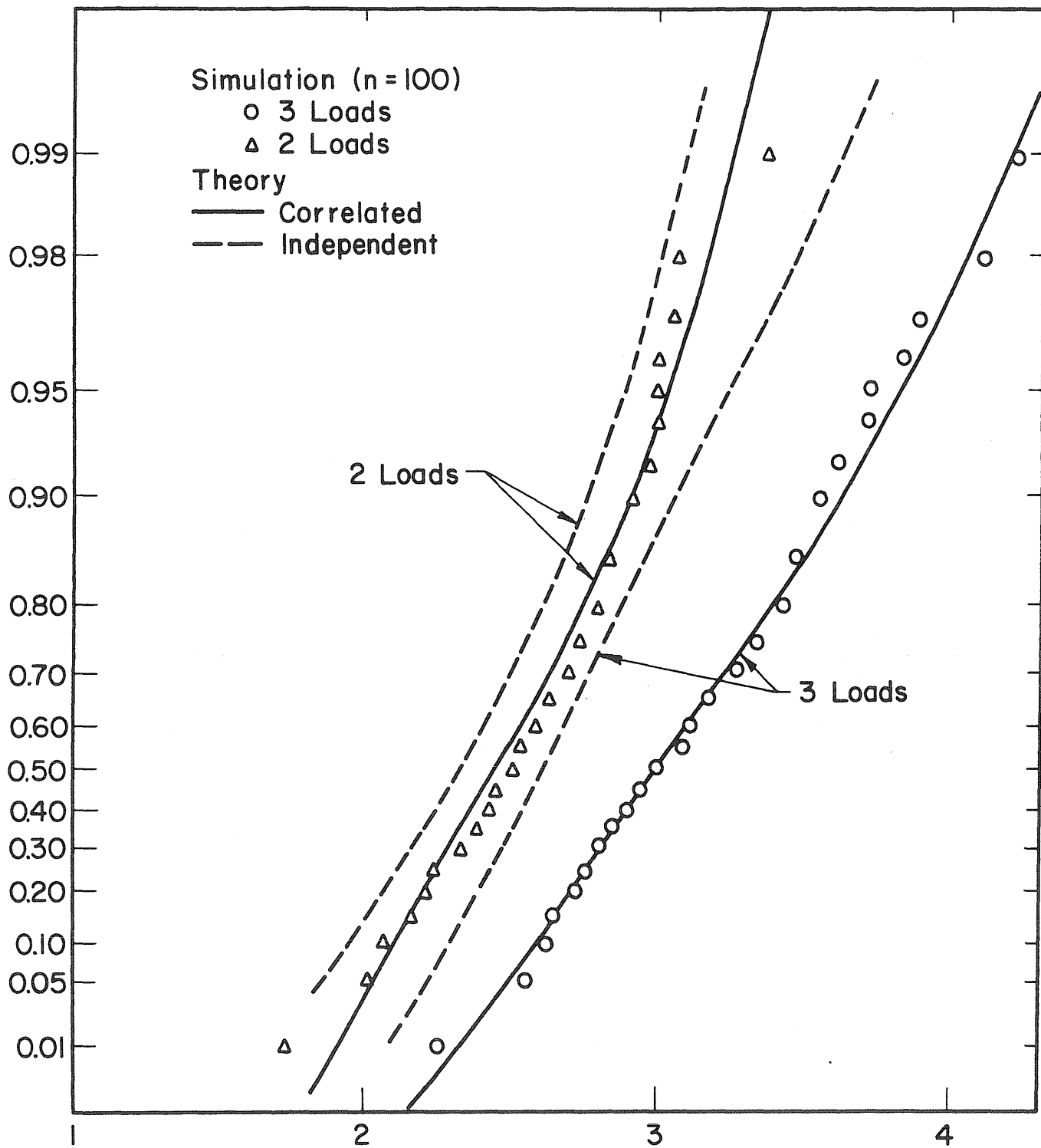


Fig. 12 Probability of Lifetime Combined Maximum  
 $(P_1=P_2=P_3=0.5, \rho_1=\rho_2=\rho_3=2, \rho=4)$

### 3.2 Intensity Dependence Between Loads

For example, storm-spawned loadings such as wind, wave and surge may have high correlation in the intensities. Such dependencies would lead to much higher probabilities of combined load level being exceeded.

The effect of such dependence is investigated using the model shown in Fig. 13. The occurrence times and load durations of the two processes are independent as in two independent Poisson renewal processes described in Section 1.1. However, intensity correlation is introduced by the conditional auto- and cross-correlation functions given that process  $S_1(t)$  and  $S_2(t)$  are "on" at the respective times. In other words, the intensity given occurrence is "sampled" from a fictitious vector continuous process (indicated by dashed lines) with a correlation matrix

$$\begin{bmatrix} R_{11}(\tau) & R_{12}(\tau) \\ R_{21}(\tau) & R_{22}(\tau) \end{bmatrix} \quad (3.23)$$

Therefore, the conditional correlation matrix of the pulse process is also described by Eq. 3.23, e.g. given that processes  $S_1(t)$  and  $S_2(t)$  are "on" at  $t_1=t_k$  and  $t_2=t_j$ , respectively,

$$E[S_1(t_k) S_2(t_j)] = R_{12}(\tau) \quad (3.24)$$

in which  $\tau=t_k-t_j$ ; the difference between the "on" times. Note that the compatibility conditions require that load processes having between-load intensity correlation have to have within-load intensity correlation.

Since the within-load dependence has only moderate effect on the life-time combined maximum (Section 2.3), it is accounted for approximately using the Gauss-Markov result previously obtained with an equivalent

$$\rho_i \approx [R_{ij}(1/\lambda_j) - E^2(x_j)] / \sigma_{x_j}^2 \quad (3.25)$$

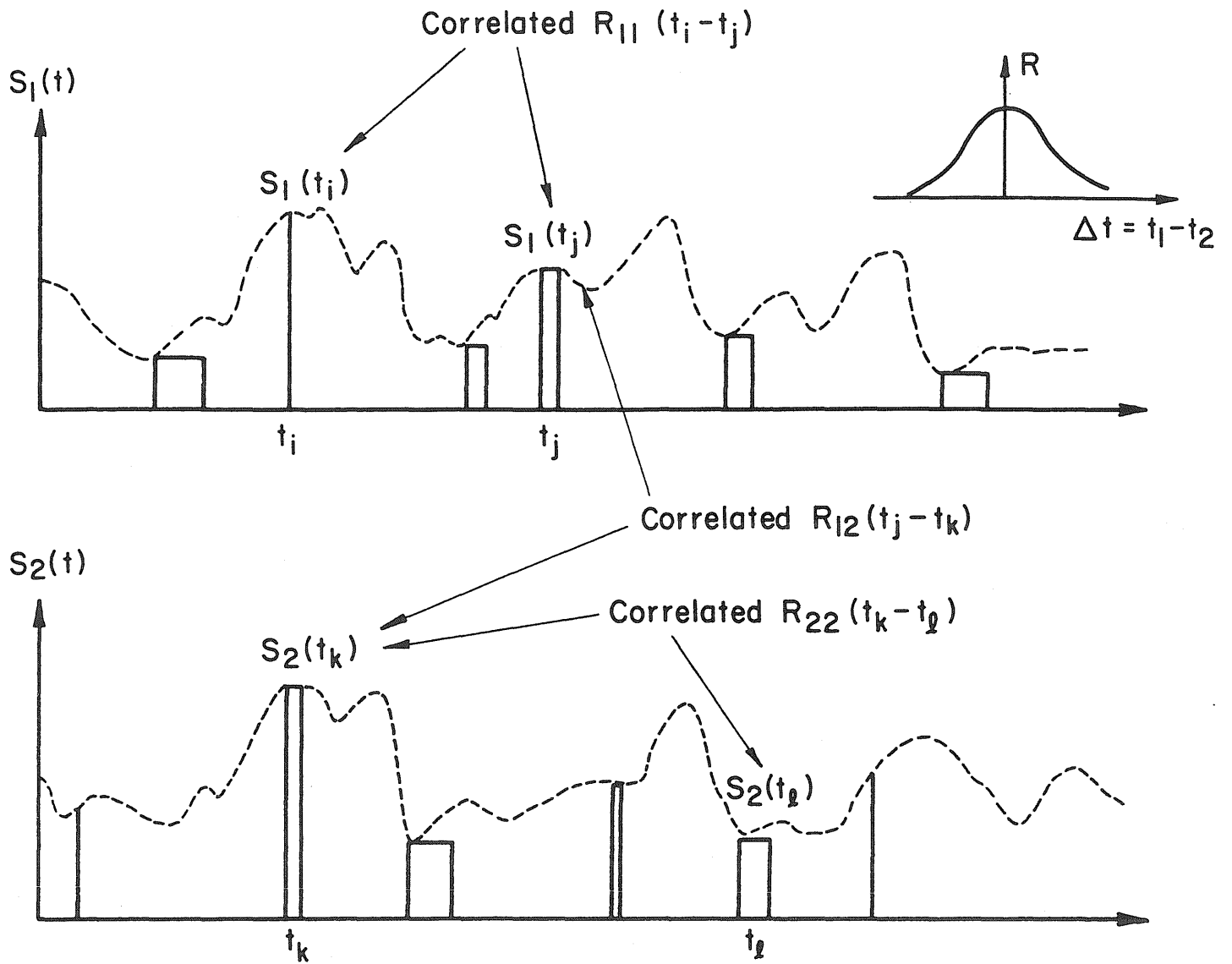


Fig. 13 Poisson Renewal Pulse Processes with Correlated Intensities

Therefore, the lifetime maximum due to individual loading has the following approximate probability distribution:

$$F_{R_i}(r, T) \approx \frac{F_{X_i}(r)}{H_i(r, \rho_i)} \exp[-v_i t H^*(r, \rho_i)] \quad (3.26)$$

Since the intensities are correlated between the loads, so are their lifetime maximum values. The combined maximum with no coincidence can be evaluated approximately from the Gumbel's type B bivariate extreme value distribution (6)

$$F_{R_1 R_2}(r_1, r_2, t) = \exp[-\{(-\ln F_{R_1}(r_1, t))^m + (-\ln F_{R_2}(r_2, t))^m\}^{1/m}] \quad (3.27)$$

in which  $m$  is a parameter specifying the correlation between the two extreme values (e.g.  $m=1$  ( $\rho=0$ ),  $m=\infty$  ( $\rho=1$ )).

Since the load occurrence time and duration are assumed to be independent, the coincidence rate  $\lambda_{12}$  is the same as that in Eq. 1.1. However, the conditional probability of threshold level being exceeded is strongly dependent on the intensity correlation between the two loads. The combined intensity depends on the time lag  $\tau$  (difference in occurrence times). Since the occurrence times are Poissonian and independent,  $\tau$  varies from  $-d_2$  to  $d_1$  (or  $-d_1$  to  $d_2$ ) with a uniform probability density function, where  $d_1$  and  $d_2$  are the load durations.

$$P(R > r | d_1, d_2) = \int_{-d_2}^{d_1} P[S_1(t) + S_2(t+\tau) > r] \frac{1}{d_1 + d_2} d\tau \quad (3.28)$$

As a first-order approximation, the condition on  $d_1$  and  $d_2$  are removed by substituting the mean values of  $d_1$  and  $d_2$  into the above equation

$$P(R > r | \text{coincidence}) = G_{12}^*(r) \approx \frac{1}{\mu_{d_1} + \mu_{d_2}} \int_{-\mu_{d_2}}^{\mu_{d_1}} P[S_1(t) + S_2(t+\tau) > r] d\tau \quad (3.29)$$

For example, if the intensities are normal variates, so is their sum.

$$P[S_1(t) + S_2(t+\tau) > r] = 1 - \Phi\left[\frac{r - (\mu_{X_1} + \mu_{X_2})}{\sqrt{\sigma_{X_1}^2 + \sigma_{X_2}^2 + 2(R_{12}(\tau) - \mu_{X_1}\mu_{X_2})}}\right] \quad (3.30)$$

Furthermore, if the load durations are much smaller than the cross-correlation time, i.e.  $\mu_{d_1}$  and  $\mu_{d_2} \ll \Delta\tau \equiv \int_0^\infty R_{12}(\tau) d\tau$ ,  $R_{12}(\tau)$  can be approximated by  $R_{12}(0)$  and Eq. 3.29 can be approximated by

$$G_{12}^*(r) \approx 1 - \Phi\left[\frac{r - (\mu_{X_1} + \mu_{X_2})}{\sqrt{\sigma_{X_1}^2 + \sigma_{X_2}^2 + 2(R_{12}(0) - \mu_{X_1}\mu_{X_2})}}\right] \quad (3.31)$$

The lifetime maximum due to coincidence is therefore governed by the probability distribution

$$F_{R_{12}}(r, T) = P(R_{12} < r, T) \approx \exp[-\lambda_{12} T G_{12}^*(r)] \quad (3.32)$$

and the overall lifetime combined maximum has the following approximate probability distribution function

$$F_{R_m}(r, T) \approx F_{R_1 R_2}(r, r, T) F_{R_{12}}(r, T) \quad (3.33)$$

To see the significance of the correlation, numerical examples based on the following correlation functions are calculated

$$\begin{aligned} R_{11}(\tau) &= \sigma_{X_1}^2 \exp[-(\tau/C_{11})^2] + \mu_{X_1}^2 \\ R_{22}(\tau) &= \sigma_{X_2}^2 \exp[-(\tau/C_{22})^2] + \mu_{X_2}^2 \\ R_{12}(\tau) &= R_{21}(\tau) = \sigma_{X_1} \sigma_{X_2} \rho \exp[-(\tau/C_{12})^2] + \mu_{X_1} \mu_{X_2} \end{aligned} \quad (3.34)$$

The conditional auto-correlations are therefore governed by  $C_{ij}$  and the cross-correlation governed by  $\rho$  and  $C_{12}$  (Note  $\rho$  and  $C_{12}$  have to satisfy certain compatibility conditions involving  $C_{11}$  and  $C_{22}$ ). Cases with parameters  $\mu_{X_1} = \mu_{X_2} = 1.0$ ,  $\sigma_{X_1} = \sigma_{X_2} = 0.3$ ,  $C_{11} = C_{22} = C_{12} = C$ ,  $\lambda_1 = \lambda_2 = \lambda$  and  $\mu_{d_1} = \mu_{d_2} = \mu_d$  and  $\rho = 0.9$  are

compared with independent loading results in Fig. 14. It is seen that at lower tail where individual loading contributions dominate, the correlation causes a lower lifetime combined maximum which agrees with findings in Section 2.3. However, as threshold level increases, the coincidence term becomes dominant and the trend is reversed, i.e., the positive correlation between the intensity causes a much higher probability of exceedance. Monte-Carlo simulations are also carried out in which a vector process is generated according to Eq. 3.34 and the method by Shinozuka and Jan (10). The comparisons are again satisfactory.

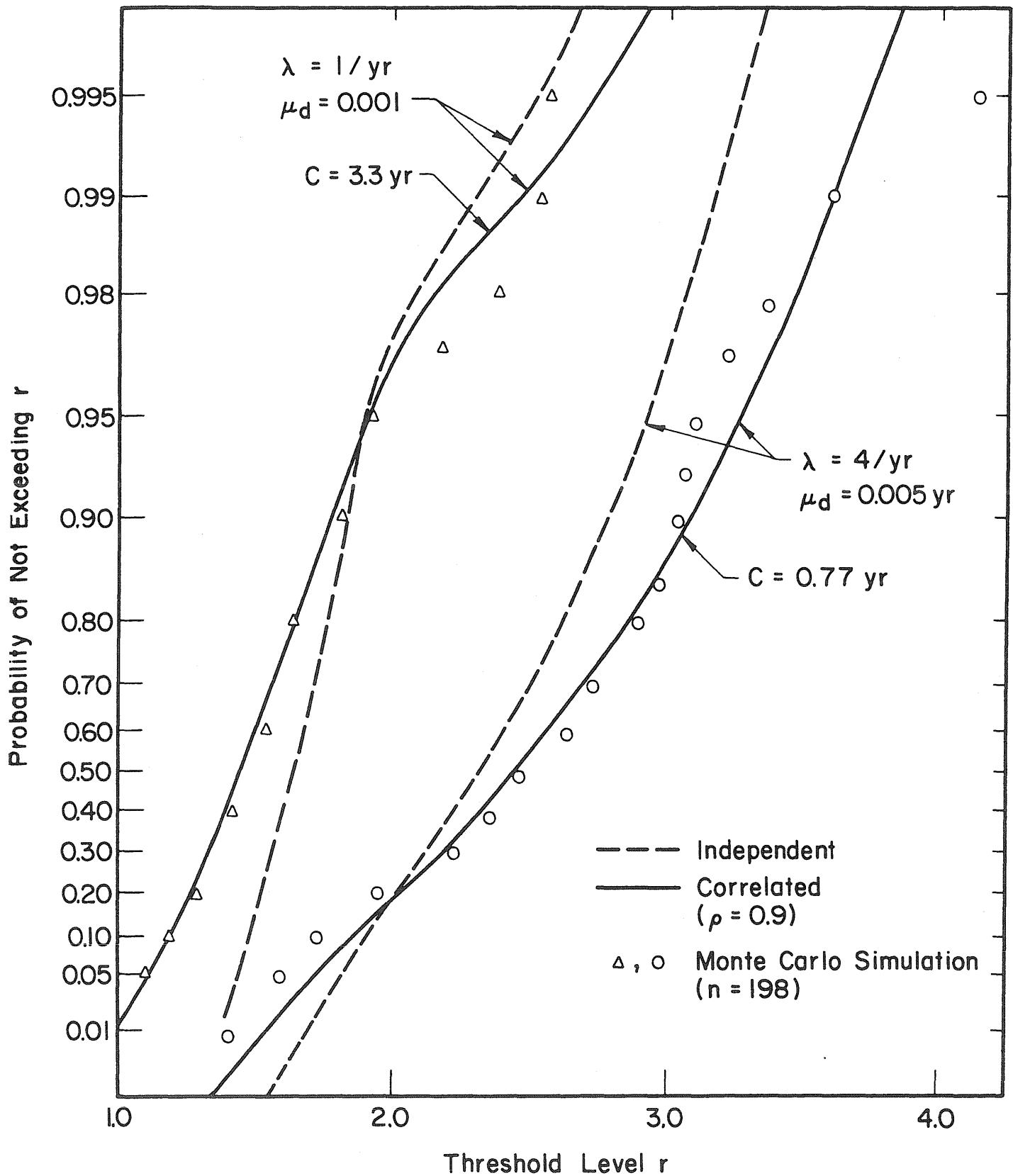


Fig. 14 Effect of Between-Load Intensity Dependence

## IV. GENERAL CASE

In general, more than one dependence can exist in the processes under combination. For example, both within-load and between-load clusterings can happen, also, the intensities of clustered, storm-spawn loadings may well be correlated. To treat such dependencies, one can properly combine the models in Sections 2 and 3. For instance, one can extend the Poisson delayed model by allowing a cluster of occurrences of load within each "on" time, (see Fig. 15). Therefore, marginally each process is of the Bartlett-Lewis type clustering process, and jointly there is a clustering of the clusters in each load around the parent point process. Thus, both within- and between-load dependencies are included.

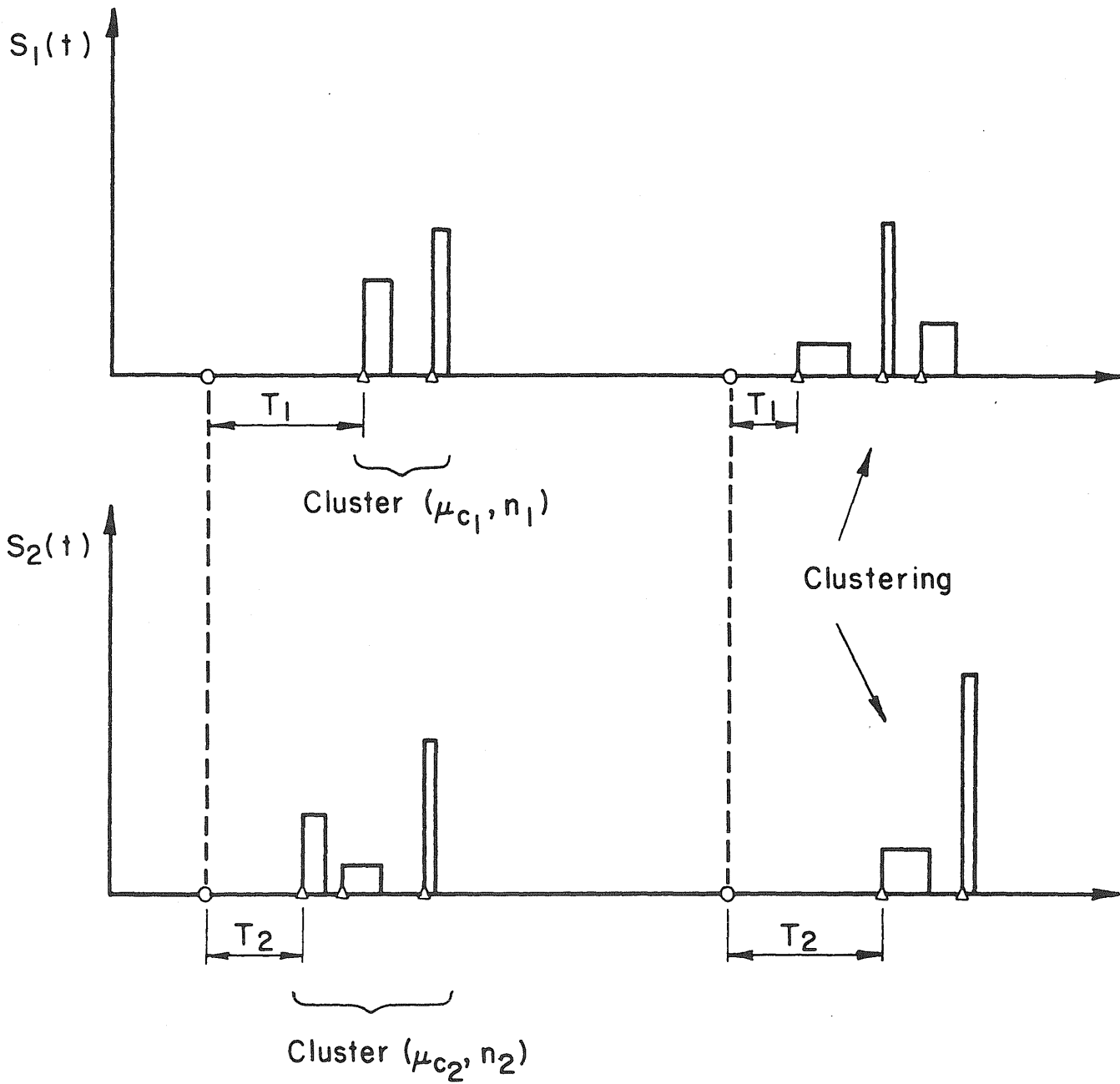
If the intensities and duration are assumed to be statistically independent as in the foregoing, an analysis similar to those given in Sections 2 and 3 would give an approximate distribution of the lifetime combined maximum

$$F_{R_m}(r, T) \approx \exp\{\lambda_1 T F_{X_1}^*(r) \left[ \frac{1}{n_1 F_{X_1}^*(r)+1} \right] + \lambda_2 T F_{X_2}^*(r) \left[ \frac{1}{n_2 F_{X_2}^*(r)+1} \right] + \lambda_{12}^c T \frac{n_1 n_2 (\mu_{d_1} + \mu_{d_2})}{(\mu_{c_1} + \mu_{c_2})} F_{X_{12}}^*(r) \left[ \frac{1}{n_1 n_2 \left( \frac{\mu_{d_1} + \mu_{d_2}}{\mu_{c_1} + \mu_{c_2}} \right) F_{X_{12}}^*(r)+1} \right]\} \quad (4.1)$$

in which  $\lambda_{12}^c$  is the mean coincidence rate of the clusters. For example, if the delay times for the cluster are modeled by exponential distribution with mean values  $a_1$  and  $a_2$ , the coincidence term in Eq. 4.1 reduces to

$$\lambda_1 \lambda_2 (\mu_{d_1} + \mu_{d_2}) \left[ 1 + \frac{p_1 p_2^0}{\lambda_1^c \lambda_2^c} \frac{1}{a_1 + a_2} \right] F_{X_{12}}^*(r) \left[ \frac{1}{n_1 n_2 \left( \frac{\mu_{d_1} + \mu_{d_2}}{\mu_{c_1} + \mu_{c_2}} \right) F_{X_{12}}^*(r)+1} \right] \quad (4.2)$$





- Parent (Generating) Point Process
- △ Delayed Clustered Point Process

Fig. 15 Within- and Between-Load Occurrence Clustering

in which  $\lambda_1^C, \lambda_2^C$  are occurrence rates of clusters.  $n$  = mean number of load occurrences in each cluster. Compared with Eq. 1.1 for the independent loadings, the two square brackets account for respectively the effects of between-load and within-load occurrence clusterings.

Similarly, when loads are correlated both in intensity and occurrences, one can combine the results given in Section 3 without difficulty, i.e. in Eq. 3.32, the coincidence rate can be replaced by that given in Eq. 3.7.

It can be seen that compared with the result for independent loadings, both the coincidence rate and the conditional probability of exceedance in this case increase considerably due to the dependencies, causing a much higher probability of exceedance at the high threshold levels. Comparisons are made in Fig. 16. The load parameters are the same as those given in Section 3.2. The additional occurrence dependence parameters are:  
 Case (I),  $\lambda_1 = \lambda_2 = \lambda = 1/\text{yr}$ ,  $\rho = 2/\text{yr}$ ,  $p_1 = p_2 = 0.5$  (i.e.  $\rho_1 = \rho_2 = 0$ ) and  $a_1 = a_2 = 0.02 \text{ yr}$ ;  
 Case (II),  $\lambda_1 = \lambda_2 = \lambda = 4/\text{yr}$ ,  $\rho = 8/\text{yr}$ ,  $p_1 = p_2 = 0.5$  ( $\rho_1 = \rho_2 = 0$ ) and  $a_1 = a_2 = .02 \text{ yr}$ . The probability distributions of lifetime (20 yrs) maximum combined load for the independent loads case are the same as those given in Fig. 14. As expected, the additional occurrence dependence gives much higher exceedance probability at the high levels.

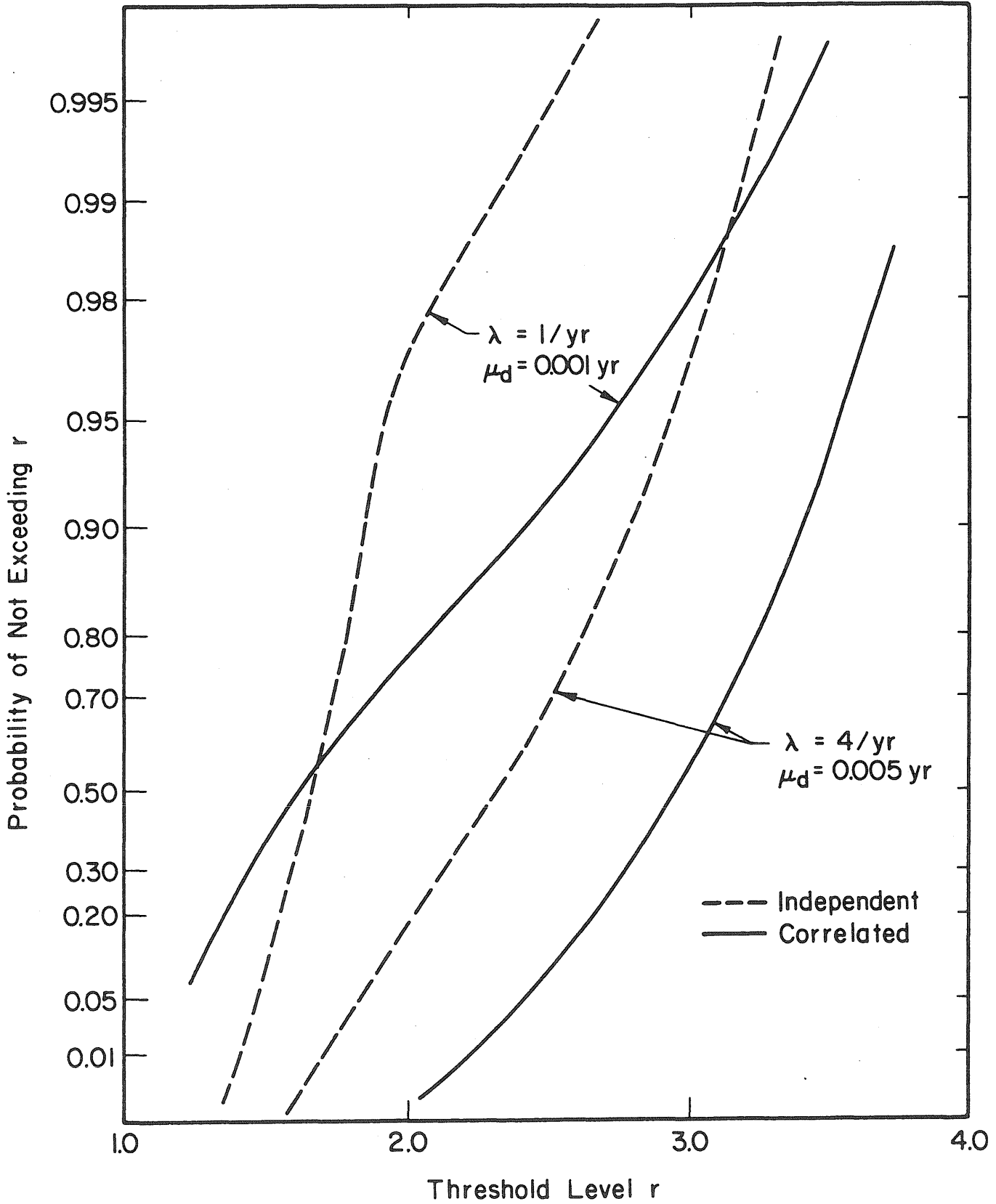


Fig. 16 Effect of Load Correlation in both Intensity and Occurrences

## V. ANALYSIS OF LOAD COINCIDENCE DURATION

When combining load effect processes using the load coincidence method, the duration of the coincidence can be an important factor; for example, when dynamic effects are considered or when structural strength deteriorates significantly with time. For loads with duration which varies from occurrence to occurrence, the load coincidence duration is also a random quantity. Experience indicates that using the mean value generally accounts satisfactorily for its variability. In the following, approximate solutions of the mean coincidence duration are obtained for the foregoing load processes.

### 5.1 Independent Loadings

It has been shown (11) that the coincidence rate for two loads is

$$\lambda_{12} \approx \lambda_1 \lambda_2 (\mu_{d_1} + \mu_{d_2}) \quad (5.1)$$

The probability that the process  $S_i(t)$  is "on" at a given time is approximately  $\lambda_i \mu_{d_i}$ . Since occurrences are independent, the probability that both processes are "on" at a given time is

$$P_{12} = \lambda_1 \lambda_2 \mu_{d_1} \mu_{d_2} \quad (5.2)$$

Let the mean duration of coincidence be  $\mu_{d_{12}}$ . It has been shown that the coincidence time is also approximately a Poisson process, therefore the probability that the coincidence process is "on" at a given time is

$$P_{12} \approx \lambda_{12} \mu_{d_{12}} \quad (5.3)$$

Substituting Eq. 5.1 into Eq. 5.3 and comparing with Eq. 5.2 one obtains

$$\lambda_{d_{12}} \approx \frac{\mu_{d_1} \mu_{d_2}}{\mu_{d_1} + \mu_{d_2}} \quad (5.4)$$

Similarly, one can show that the mean duration of coincidence of three loads is

$$\lambda_{d_{123}} \approx \frac{\mu_{d_1} \mu_{d_2} \mu_{d_3}}{\mu_{d_1} \mu_{d_2} + \mu_{d_1} \mu_{d_3} + \mu_{d_2} \mu_{d_3}} \quad (5.5)$$

The result given in Eq. 5.4 can be derived from a different approach. Given the durations being  $d_1$  and  $d_2$ , the duration of the overlap  $D_0$  is a function of the difference in occurrence times  $\tau$  (see Fig. 17). Since the occurrence times of  $S_1(t)$  and  $S_2(t)$  are Poisson and independent,  $\tau$  is uniformly distributed between  $-d_1$  and  $d_2$  is therefore,

$$\begin{aligned} E[D_0 | d_1, d_2] &= \int D_0(\tau) f(\tau) d\tau \\ &= \frac{1}{d_1 + d_2} \int_{-d_1}^{d_2} D_0(\tau) d\tau \\ &= \frac{d_1 d_2}{d_1 + d_2} \quad \text{for } d_2 > d_1 \end{aligned} \quad (5.6)$$

The same result can be obtained for  $d_2 < d_1$ .

Using the first order approximation

$$E[D_0] = \mu_{d_{12}} \approx \frac{\mu_{d_1} \mu_{d_2}}{\mu_{d_1} + \mu_{d_2}} \quad (5.7)$$

## 5.2 Dependent Loadings

The overlap duration would be affected by the dependence only if the dependences are in the occurrence times and durations. Consider first the case of within-load occurrence clustering. Coincidence of loadings happens

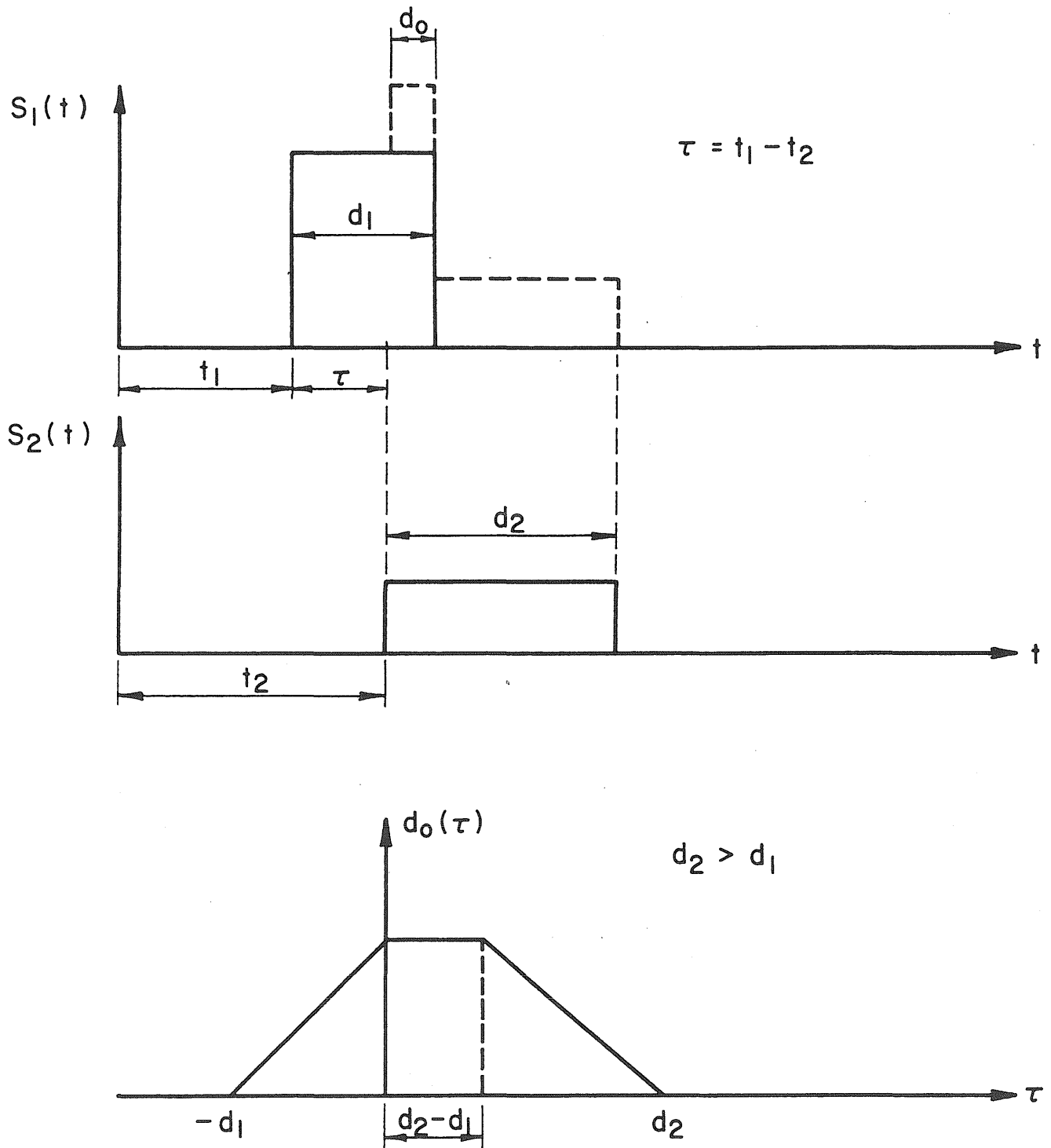


Fig. 17 Coincidence Duration for Independent Pulse Processes

only when there is a coincidence of the clusters and within the clusters, the loadings occur according to Poisson processes. Since the two loading processes are independent, the analysis of the duration of the coincidence would be the same as the unclustered case except that the difference in occurrence time  $\tau$  may not be exactly a uniformly distributed random variable because of the clustering. However, from Eq. 5.6 one can see that  $E[D_0|d_1, d_2]$  is not very sensitive to a slight change in the density function of  $\tau$ . Therefore, one has reason to believe Eq. 5.7 can be used as a good approximation; this point will be further supported by the following analysis.

When between-load occurrence clustering exists the mean coincidence duration would be affected by the dependences. For example, one would expect that Eq. 5.4 can still be used as a good approximation when the dependence is weak, and the mean duration would be much longer when the dependence is strong. Following an analysis similar to that given in Eqs. 5.1 to 5.4, the mean duration is obtained as follows.

Given the durations  $d_1$  and  $d_2$ , the process  $S_1(t)$  is "on" at a given time  $t=t_0$  if (see Fig. 18)  $0 \leq \xi_1 \leq d_1$ . Similarly,  $S_2(t)$  is "on" at  $t=t_0$  if  $0 \leq \xi_2 \leq d_2$ . The probability that both loads are "on" at  $t=t_0$  is

$$P_{12} = P(0 \leq \xi_1 \leq d_1 \cap 0 \leq \xi_2 \leq d_2) \quad (5.8)$$

Since the occurrence times are now correlated, so are  $\xi_1$  and  $\xi_2$ . The joint density function of  $\xi_1$  and  $\xi_2$  is

$$f_{\xi_1 \xi_2} = f_{\xi_2 | \xi_1} f_{\xi_1} \quad (5.9)$$

in which  $f_{\xi_1} = \lambda_1 e^{-\lambda_1 \xi_1}$  since marginally, the occurrence time of  $S_1(t)$  follows a Poisson distribution (Section 3.1). Making use of the conditional

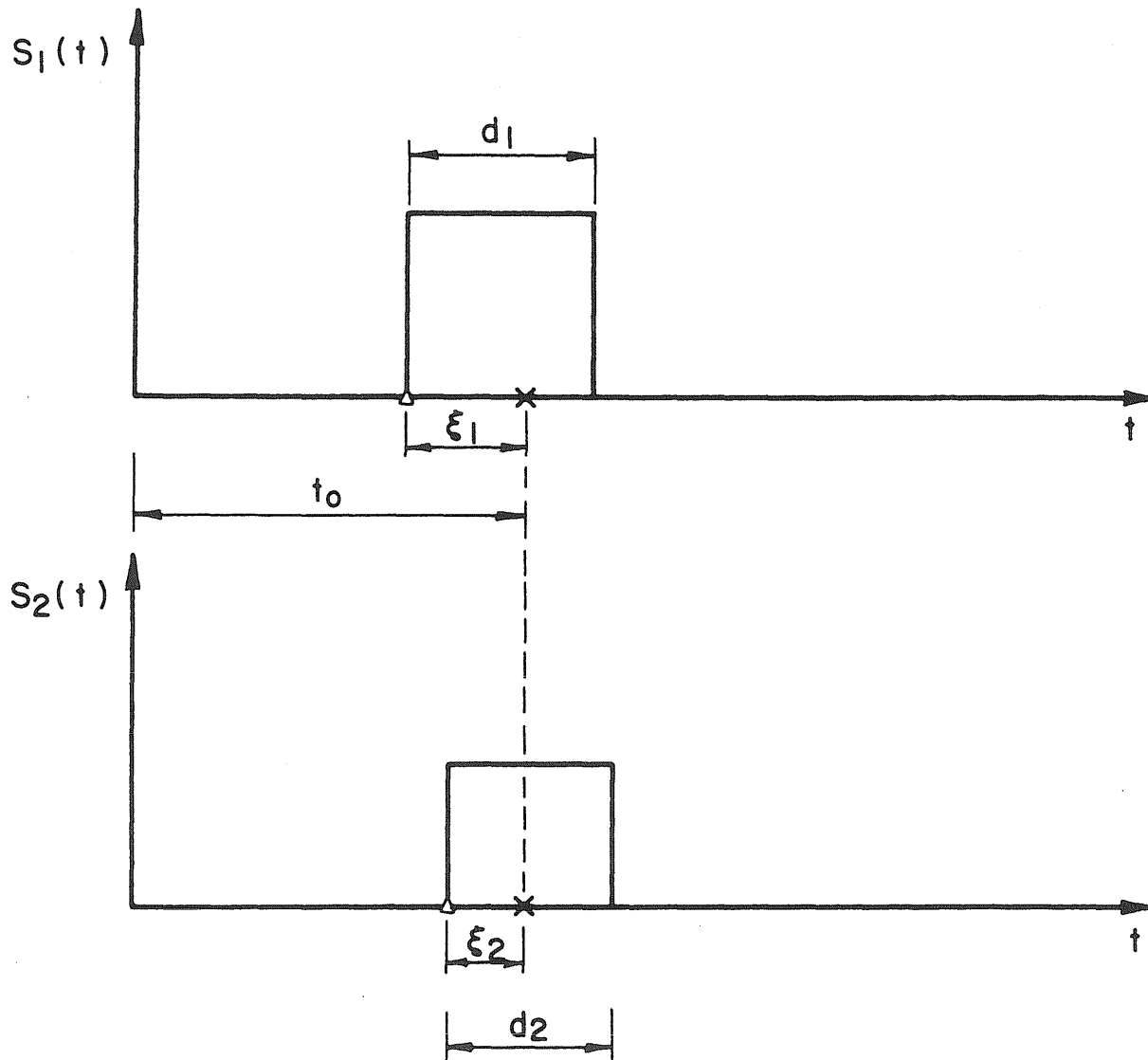


Fig. 18 Condition that Process  $S_1(t)$  and  $S_2(t)$  are "on" at  $t=t_0$



occurrence rate function (C.O.R.) defined in Eq. 3.1

$$\begin{aligned}
 f_{\xi_2|\xi_1} &= \frac{d}{d\xi_2} \left[ 1 - e^{-\int_0^{\xi_1-\xi_2} h_1^{(2)}(\tau) d\tau} \right] \\
 &= e^{-\int_0^{\xi_1-\xi_2} h_1^{(2)}(\tau) d\tau} h_1^{(2)}(\xi_1-\xi_2)
 \end{aligned} \tag{5.10}$$

Therefore,

$$P_{12} = \int_0^{d_1} \int_0^{d_2} f_{\xi_2|\xi_1} f_{\xi_1} d\xi_2 d\xi_1 \tag{5.11}$$

If  $\lambda_j d_j \ll 1$  (transient loads) the two exponential functions in Eq. 5.11 are approximately equal to unity

$$\begin{aligned}
 P_{12} &\approx \int_0^{d_1} \int_0^{d_2} \lambda_1 h_1^{(2)}(\xi_1-\xi_2) d\xi_1 d\xi_2 \\
 &= \lambda_1 \lambda_2 d_1 d_2 + \rho P_1 P_2 \int_0^{d_2} \int_0^{d_1} f_{T_2-T_1}(\xi_1-\xi_2) d\xi_1 d\xi_2
 \end{aligned} \tag{5.12}$$

The conditions on  $d_1$  and  $d_2$  can be removed by using the mean values  $\mu_{d_1}$  and  $\mu_{d_2}$  in Eq. 5.12 as an approximation.

In Section 3.1 it has been shown that the coincidence is also a Poisson process with a mean occurrence rate  $\lambda_{12}$  given by Eq. 3.7. Let  $\mu_{d_{12}}$  be the mean duration of coincidence, the probability that the coincidence process is "on" at a given time is

$$P_{12} \approx \lambda_{12} \mu_{d_{12}}$$

Comparing with Eq. 5.12, one obtains

$$\mu_{d_{12}} \approx \frac{1}{\mu_{12}} [\lambda_1 \lambda_2 \mu_{d_1} \mu_{d_2} + \rho P_1 P_2 \int_0^{\mu_{d_2}} \int_0^{\mu_{d_1}} f_{T_2-T_1}(\xi_1 - \xi_2) d\xi_1 d\xi_2] \quad (5.13)$$

If  $P_1$  or  $P_2=0$ , the clustering disappears  $\mu_{d_{12}}$  reduces to that in Eq. 5.4 as it should. The sensitivity of increase in  $\mu_{d_{12}}$  due to occurrence clustering as compared with Eq. 5.4 is shown in Table 6 for the case  $\rho=\lambda_1=\lambda_2=2/\text{yr}$  ( $\rho_1=\rho_2=0$ ,  $P_1=P_2=1$ ),  $\mu_{d_1}=\mu_{d_2}=\mu_d=0.001 \text{ yr}$  (8 hrs) and exponential delay times with mean values  $a_1=a_2=a$ . It is seen that if the ratio of mean duration to mean delay time  $\mu_d/a$  is small, Eq. 5.4 can be used as a good approximation. Similarly, one can show that the mean duration of coincidence of three loads with possible between-load occurrence clustering is

$$\mu_{d_{123}} \approx \frac{1}{\lambda_{123}} [\lambda_1 \int_0^{\mu_{d_3}} \int_0^{\mu_{d_2}} \int_0^{\mu_{d_1}} h_{12}^{(3)}(\xi_1 - \xi_3, \xi_1 - \xi_2) h_1^{(2)}(\xi_1 - \xi_2) d\xi_3 d\xi_2 d\xi_1] \quad (5.14)$$

in which  $\lambda_{123}$  is given by Eq. 3.17.

TABLE 6 Mean Coincidence Duration

$\mu_d/a$	Eq. 5.4	Eq. 5.13
.1	.0005 yr	.000513 yr
.5	.0005 yr	.000645 yr
1.0	.0005 yr	.000732 yr
5.0	.0005 yr	.000926 yr

## VI. SUMMARY AND CONCLUSION

Because of the transient and intermittent nature of most environmental loadings on structures, general treatment of the stochastic dependence in load combination analysis is difficult. In this study, models based on pulse load processes are developed in which load occurrence time, intensity and duration may be correlated within each process and between processes. The occurrence time dependence is modeled by multi-variate clustering point process and intensity and duration dependence by Gauss-Markov sequence, conditional correlation functions and multi-variate distributions. The effect of dependencies are investigated in the context of the lifetime maximum of the summation of two load processes. The load coincidence method previously proposed for combination of independent loading is generalized for dependent loadings and approximate solutions are obtained in simple, closed form and verified by Monte-Carlo simulations. It is found that compared with results for independent loadings:

(1) Within-load duration-intensity correlation causes a slight increase in the exceedance probability for lifetime combined maximum at the high threshold level;

(2) Within-load intensity dependence and occurrence clustering cause a moderate decrease in such probability in the lower tail and have little effect at the high threshold level;

(3) Load coincidence rate is extremely sensitive to the between-load occurrence clustering, increases of several orders of magnitude could result giving much higher probability of exceedance at the high threshold level;

(4) Between-load intensity correlation is important at the high threshold level; and

(5) When both intensity and occurrence dependences exist between loads, the effects are multiplicative causing an extremely high probability of exceedance at the high threshold level.

The above conclusions hold for linear combination of load effect processes which can be reasonably represented by pulse processes, such as static or equivalent static load effects. For nonlinear and dynamic systems, the coincidence rate and cluster analysis remain valid, however, the analysis of conditional probability of failure becomes more involved requiring more detail modeling of the excitation given occurrence and structural response behavior, such as reliability and random vibration analyses (12). This is currently under investigation. Findings will be given in a subsequent report.

## REFERENCES

1. Bartlett, M.S., "The Spectral Analysis of Point Processes," Journal of Royal Statist. Soc., B25, pp. 264-296.
2. Cox, D.R. and Lewis, P.A.W., "Multi-Variate Point Process," Proc. 6th Berkeley Symposium on Mathematical Statistics, 1972, Proc. 3, pp. 401-448.
3. Cox, D.R., Renewal Theory, Methuen and Co., London, 1962.
4. Feller, W., An Introduction to Probability Theory and Its Applications, Vol. II, John Wiley and Sons, Inc., New York, 1966.
5. Grigoriu, M. and Turkstra, C., "Structural Safety Indices for Repeated Loads," Journal of the Engineering Mechanics Division, ASCE, Vol. 104, No. EM4, August, 1978.
6. Johnson, N.L. and Kotz, S., Distributions in Statistics: Continuous Multi-Variate Distributions, John Wiley and Sons, Inc., 1972.
7. Larrabee, R.D., "Approximate Stochastic Analysis of Combined Loading," Res. Rep. CER78-28, M.I.T., September, 1978.
8. Madsen, H., Kilcup, R., and Cornell, C.A., "Mean Upcrossing Rate for Sums of Pulse-Type Stochastic Load Processes," Proc. ASCE Specialty Conference on Probabilistic Mechanics and Structural Reliability, Tucson, Arizona, January, 1979.
9. Ravindra, M.K., "Load Combination for Natural and Man-Made Hazards in Nuclear Structural Design," A.N.C. Conference on Thermal Reactor Safety, Sun Valley, Idaho, July 31, 1977.
10. Shinozuka, M. and Jan, C.M., "Digital Simulation of Random Processes and Its Applications," Journal of Sound and Vibration, Vol. 25, No. 1, 1972, pp. 11-128.
11. Wen, Y.K., "Statistical Combination of Extreme Loads," Journal of Structural Division, ASCE, Vol. 103, No. ST5, May, 1977.
12. Wen, Y.K., "Methods for Reliability of Structures under Multiple Time Varying Loads," Nuclear Engineering and Design 60 (1980), pp. 61-71.
13. Wen, Y.K., "Reliability Analysis under the Combination of Stochastic Loads," Proc. International Specialty Conference on the Probabilistic Safety of Structures, September 8-9, 1980, Paris, France.

Appendix A: Sum of Two Independent Gauss-Markov Processes

Let  $\{x\} = X_1, X_2, \dots, X_n$  and  $\{y\} = Y_1, Y_2, \dots, Y_n$  be two independent stationary Gauss-Markov sequences with one-step correlation coefficients  $\rho_X$  and  $\rho_Y$ , respectively. Let  $\{S\} = S_1, S_2, \dots, S_n$  be the sum process. It can be shown that the correlation coefficient between  $S_i$  and  $S_k$  is

$$\rho_{S_i S_k} = \frac{\sigma_X^2 \rho_X^{|k-i|} + \sigma_Y^2 \rho_Y^{|k-i|}}{\sigma_X^2 + \sigma_Y^2} \quad (\text{A-1})$$

From Ref. 4  $\{S\}$  is a Gauss-Markov sequence if and only if

$$\rho_{S_i S_k} = \rho_S^{|k-i|} \quad (\text{A-2})$$

in which  $\rho_S$  = one-step correlation coefficient.

It is seen that Eq. A-1 reduces to Eq. A-2 only when  $\rho_X = \rho_Y$ . However, comparison of Eqs. A-1 and A-2 shows that (Fig. 19) even when  $\rho_X \neq \rho_Y$  the difference is not very large; therefore, the Markov Process can be used as an approximation.

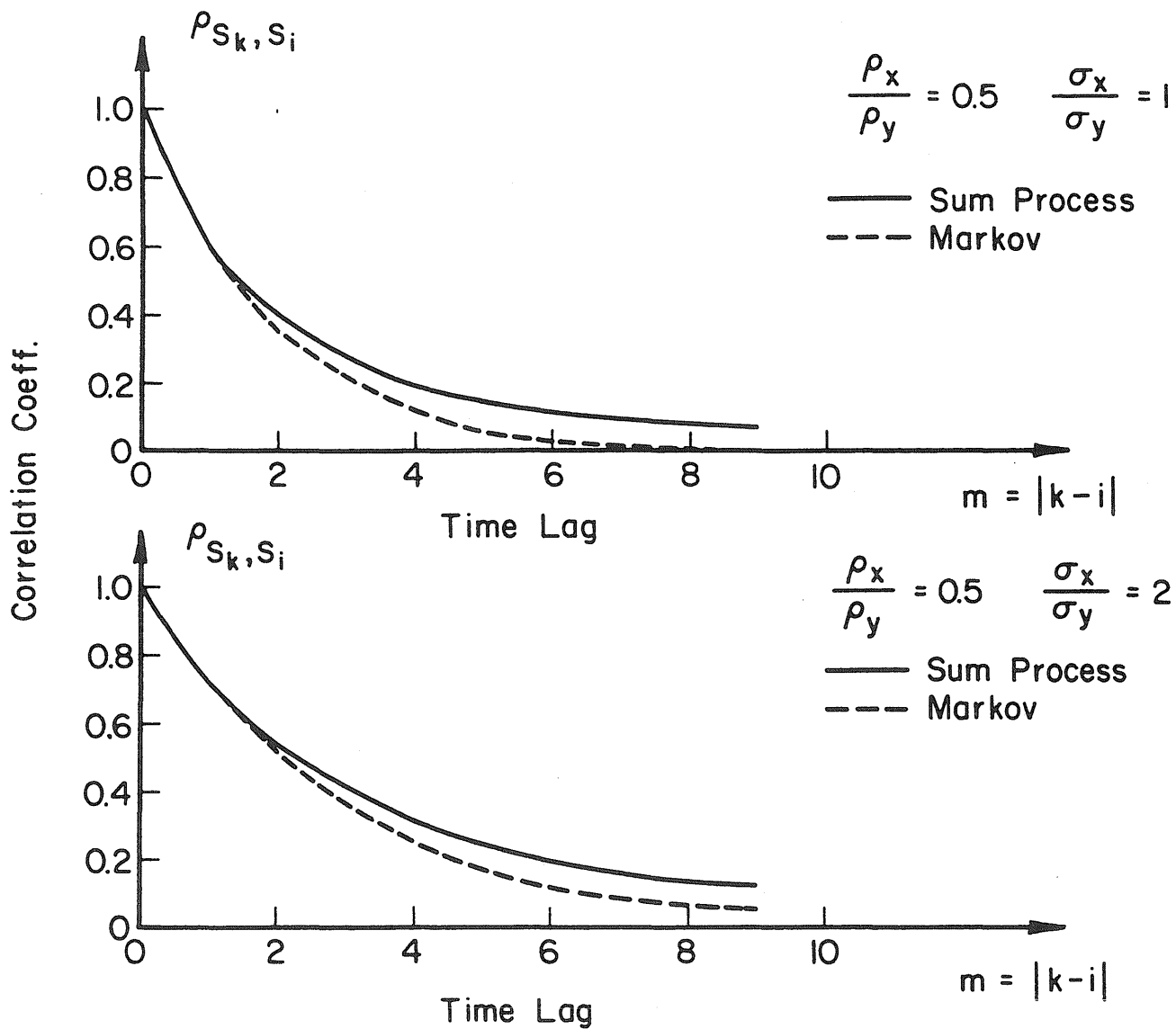


Fig. 19 Comparison of Correlation Coefficient Functions



Appendix B: Derivation of Function  $h_{12}^{(3)}(t, t')$

Define a 3-D extension of  $\gamma_1^{(2)}$  in Eq.

$$\gamma_{123}(t, t') = \lim_{\Delta' t, \Delta'' t, \Delta''' t \rightarrow 0} \frac{1}{\Delta' t \Delta'' t \Delta''' t} E\{[N^{(1)}(0, \Delta' t) - E(N^{(1)})][N^{(2)}(t', t' + \Delta'' t) - E(N^{(2)})][N^{(3)}(t, t + \Delta''' t) - E(N^{(3)})]\} \quad (B-1)$$

Expanding the product within the expectation one obtains:

$$\begin{aligned} \gamma_{123}(t, t') = \lim_{\Delta' t, \Delta'' t, \Delta''' t \rightarrow 0} \frac{1}{\Delta' t \Delta'' t \Delta''' t} \{ & E(N^{(1)} N^{(2)} N^{(3)}) - E(N^{(1)} N^{(2)}) \\ & E(N^{(3)}) - E(N^{(2)} N^{(3)}) E(N^{(1)}) - E(N^{(1)} N^{(3)}) E(N^{(2)}) + 2E(N^{(1)}) E(N^{(2)}) \\ & E(N^{(3)}) \} \end{aligned} \quad (B-2)$$

Using the definition of COR functions and  $\lambda_i$

$$\begin{aligned} \gamma_{123}(t, t') = \lim_{\Delta' t, \Delta'' t, \Delta''' t \rightarrow 0} \frac{1}{\Delta' t \Delta'' t \Delta''' t} \{ & \lambda_1 \Delta' t h_1^{(2)}(t') \Delta'' t h_{12}^{(3)}(t, t') \Delta''' t \\ & - \lambda_1 \Delta' t h_1^{(2)}(t') \Delta'' t \lambda_3 \Delta''' t - \lambda_2 \Delta'' t h_2^{(3)}(t-t') \Delta''' t \lambda_1 \Delta' t - \lambda_1 \Delta' t h_1^{(3)}(t) \Delta''' t \lambda_2 \Delta'' t \\ & + 2\lambda_1 \Delta' t \lambda_2 \Delta'' t \lambda_3 \Delta''' t \} \end{aligned} \quad (B-3)$$

The time increments cancel with denominator. Solve for  $h_{12}^{(3)}(t, t')$ , one obtains Eq.

From the definition of  $\gamma_{123}$  it is clear that components in  $S_1(t)$ ,  $S_2(t)$  and  $S_3(t)$  which are statistically independent have no contribution to  $\gamma_{123}$ . Since all the "noise" parts of the processes are statistically independent and independent of the parent and delayed processes, unless all three points have the same cluster center, at least one point is independent of the other two and the contribution to  $\gamma_{123}$  would be zero.

Therefore, an extension of Eq.

$$\begin{aligned}
 \gamma_{123}(t, t') &= \lim_{\Delta t, \Delta t', \Delta t'' \rightarrow 0} \rho P_1 \Delta t P[t' < T_2 - T_1 < t' + \Delta t', \\
 &\quad t < T_3 - T_1 < t + \Delta t''] P_2 P_3 / \Delta t \Delta t' \Delta t'' \\
 &= \rho P_1 P_2 P_3 \int_0^{\infty} f_{T_2}(t' + \tau) f_{T_3}(t + \tau) f_{T_1}(\tau) d\tau
 \end{aligned} \tag{B-4}$$

Appendix C: Integration of Eq. 3.15

For exponential delay time distributions, substituting Eqs. 3.5 and 3.12 into Eq. 3.15 gives

$$H_{23} = \begin{cases} C_1 & \text{for } d_1 \leq d_2 \\ C_1 - C_2 & \text{for } d_1 > d_2 \end{cases}$$

$$\begin{aligned} C_1 = \frac{\rho}{\lambda_1} & \left\{ \frac{P_1 P_2 P_3}{(a_1 a_2 + a_2 a_3 + a_1 a_3)} a_3 \left[ \frac{a_2 a_3}{(a_2 + a_3)} (1 - e^{-d_1 (\frac{1}{a_2} + \frac{1}{a_3})}) - a_2 e^{-d_1/a_3} \right. \right. \\ & (1 - e^{-d_1/a_2}) \left. \left. \right] + \frac{\lambda_1 P_2 P_3}{(a_2 + a_3)} a_3 [d_1 - a_3 (1 - e^{-d_1/a_3})] \right. \\ & + \frac{\lambda_2 P_1 P_3}{(a_1 + a_3)} a_3 [a_3 - (a_3 + d_1) e^{-d_1/a_3}] + \frac{\lambda_3 P_1 P_2}{(a_1 + a_2)} a_2 [d_1 - a_2 (1 - e^{-d_1/a_2})] \left. \right\} \\ & + \lambda_2 \lambda_3 \frac{d_1^2}{2} \end{aligned} \quad (C-1)$$

$$\begin{aligned} C_2 = \frac{\rho}{\lambda_1} & \left\{ \frac{P_1 P_2 P_3}{(a_1 a_2 + a_2 a_3 + a_1 a_3)} a_3 \left[ \frac{e^{-d_2/a_3}}{(1/a_2 + 1/a_3)} (1 - e^{-(d_1 - d_2)(1/a_2 + 1/a_3)}) \right. \right. \\ & - a_2 e^{-d_1/a_3} (1 - e^{-(d_1 - d_2)/a_2}) \left. \left. \right] + \frac{\lambda_1 P_2 P_3}{(a_2 + a_3)} a_3 [(d_1 - d_2) e^{-d_2/a_3} - e^{-d_1/a_3} \right. \\ & a_3 (e^{(d_1 - d_2)/a_3} - 1)] + \frac{\lambda_2 P_1 P_3}{(a_1 + a_3)} a_3 [a_3 (e^{-d_2/a_3} - e^{-d_1/a_3}) - (d_1 - d_2) \\ & e^{-d_1/a_3}] + \frac{\lambda_3 P_1 P_2}{(a_1 + a_2)} a_2 [(d_1 - d_2) (1 - e^{-(d_1 - d_2)/a_2}) - (a_2 - e^{-(d_1 - d_2)/a_2} \\ & (d_1 - d_2 + a_2))] \left. \right\} + \lambda_2 \lambda_3 \frac{(d_1 - d_2)^2}{2} \end{aligned} \quad (C-2)$$

## Appendix D: Monte-Carlo Simulation and Combination of Dependent Pulse Processes

In order to demonstrate the method of simulating the loads on a structure over its lifetime, the general technique of the Monte-Carlo simulation is first described. The specific methods used when considering dependencies within and between loads are considered thereafter.

### General Simulation Methods

The computer is capable of performing thousands of operations each second. Therefore, if we are able to accurately model an experiment or series of events on the computer, we can obtain sufficient data, in a short time, to enable us to analyze the statistics of the experiment.

One of the most important tools for this type of simulation is a random number generator. The basic one which is sure to be found on all computers is that which generates random number uniformly distributed between 0. and 1. However, we may require random variables in the simulation which have distributions other than uniform. To obtain these variates we use a well known technique.

An example is given to illustrate the technique for exponentially distributed random variables  $\{X_i\}$  whose distribution function is given by  $F(X) = 1 - \exp(-\lambda X)$ .

A set of random variates  $\{U_i\}$  uniformly distributed between 0. and 1. is generated. The  $\{X_i\}$  are obtained from the inverse of the distribution function

$$U_i = F(X_i) = 1 - \exp(-\lambda X_i)$$

$$\Rightarrow \exp(-\lambda X_i) = 1 - U_i$$

$$\Rightarrow X_i = -\frac{1}{\lambda} \ln(1-U_i)$$

### Poisson Renewal Pulse Process

This study requires the simulation of load processes such as those shown in Fig. 1. The occurrence of the loads is a Poisson process which means that the times between occurrences are exponentially distributed. These occurrence times  $\{t_i\}$  may therefore be easily simulated by first simulating the times between loads  $\{d_i\}$ .

Starting condition; no load at  $t=0$

$t_k$  = time of occurrence at  $k$ th load

$d_i$  = time between occurrence of  $i-1$  and  $i$ th load

$$\Rightarrow t_k = \sum_{i=1}^k d_i$$

The duration of the loads is also taken to be exponentially distributed.

They may be simulated in two ways.

- i) Having obtained the occurrence times of the loads, the simulated durations are merely added to each of the starting times. This method has the disadvantage of producing a probability (although small) of overlap of two loads.
- ii) Rather than simulating occurrence times of the loads, generate many points whose mean interval is the same as the mean load duration. There is then a probability of these new "loads" having zero intensity. This probability is given by

$$P(0) = 1 - \lambda \mu_D$$

where  $\lambda$  = mean rate of arrival of loads

$\mu_D$  = mean load duration.

To choose those loads which will have a non-zero intensity, generate uniform random numbers between 0. and 1. each being designated to a load occurrence. Those loads whose designated random variate is less than or equal to  $\lambda \mu_D$  will be considered the real loads on the structure. They will have a mean arrival rate of  $\lambda$  and a mean duration of  $\mu_D$ .

Thus far, the start- and end-times of each load occurrence of a particular load-type are stored in the computer. For each occurrence it is then an easy matter to generate a load intensity from knowledge of its probability distribution.

Present interest is in the combined occurrence of at least two load types as described above. It is therefore necessary to generate and store two statistically independent loads occurring over the lifetime of the structure. Once this is done, the values needed for the statistics are obtained by counting the number of times overlaps (or coincidences) occur between the two load types and searching for the maximum combined load on the structure during its life.

The procedure as described above is repeated, with new independent load processes, until enough observations have been obtained to give reliable statistics.

#### Within-Load Dependencies

1. Occurrence Clustering. This is a simple extension of the above simulation procedure. The process to be generated is shown in Fig. 3.

The start- and end-times of the clusters are generated in similar fashion to those of the loads described above. Then all that is required is for the individual loads to be generated within each cluster, given the mean number per cluster and the mean load duration.

2. Intensity Dependence. The generation of the times of occurrence of loads is the same as that of the Poisson renewal pulse process. The only difference now is that the intensities of the loads are not independent within each load case.

The intensities are generated as a dependent sequence, the details of which are given on page 15.

#### Between-Load Dependencies

1. Occurrence Clustering among Loads. Such processes are illustrated in Fig. 7. There are now two processes being superimposed to form the one load case. The first is termed a delayed point process and the second an

independently and superimposed on the above.

To obviate any overlapping of loads within each load case, a new process is generated with mean occurrence rate

$$\frac{1}{\mu_d} = P\lambda + \nu$$

where,

$\mu_d$  = mean load duration

$P$  = probability of occurrence of delayed process

$\lambda$  = occurrence rate of parent process

$\nu$  = occurrence rate of noise process

The end-times of the load occurrences are then given by the new process after each load occurrence time, for both noise and delayed loads.

2. Intensity Dependence Between Loads. The load occurrences and durations are independent and are generated as for the Poisson renewal pulse process. As described in page 44, the intensities of the correlated processes are obtained by "sampling" a fictitious continuous vector process at the times of occurrence of the individual loads.

The correlation matrix for the vector process must be given. Details of the procedure used to simulate the vector process may be found in the paper by Shinozuka and Jan (10).

